

Tailored intestinal IgA responses can set an evolutionary trap for *Salmonella* Typhimurium

Médéric Diard^{1,2,*}, Erik Bakkeren¹, Daniel Hoces³, Verena Lentsch³, Markus Arnoldini³, Flurina Böhi^{1,17}, Kathrin Schumann-Moor^{1,19}, Jozef Adamcik³, Luca Piccoli⁴, Antonio Lanzavecchia⁴, Beth M. Stadtmueller⁵, Nicholas Donohue^{6,18}, Marjan W. van der Woude⁶, Alyson Hockenberry^{7,8}, Patrick H. Viollier⁹, Laurent Falquet^{10,11}, Daniel Wüthrich¹², Ferdinando Bonfiglio¹³, Claude Loverdo¹⁵, Adrian Egli^{12,13}, Giorgia Zandomenighi¹⁴, Raffaele Mezzenga^{3,15}, Otto Holst¹⁶, Beat H. Meier¹⁴, Wolf-Dietrich Hardt^{1,*}, Emma Slack^{1,3,*}

Affiliations;

1. Institute for Microbiology, Department of Biology, ETH Zürich, Zürich, Switzerland
2. Biozentrum, University of Basel, Basel, Switzerland
3. Institute for Food, Nutrition and Health, ETH Zürich, Zürich, Switzerland
4. Institute for Research in Biomedicine, Università della Svizzera italiana, Bellinzona, Switzerland
5. Department of Biochemistry, University of Illinois at Urbana-Champaign, Urbana, Illinois USA
6. York Biomedical Research Institute, Hull York Medical School, University of York, York, UK
7. Department of Environmental Microbiology, Eawag, Dübendorf, Switzerland
8. Department of Environmental Sciences, ETH Zürich, Switzerland
9. Microbiology and Molecular Medicine, University of Geneva, Geneva, Switzerland
10. Department of Biology, University of Fribourg, Fribourg, Switzerland
11. Swiss Institute of Bioinformatics, Fribourg, Switzerland
12. Infection Biology, Basel University Hospital, Basel, Switzerland
13. Department of Biomedicine, University of Basel, Basel, Switzerland
14. Institute for Physical Chemistry, ETH Zürich, Zürich, Switzerland
15. ETH Zürich, Department of Materials, Wolfgang-Pauli-Strasse 10, 8093 Zürich.
16. Forschungszentrum Borstel, Borstel, Germany

Current addresses:

17. Department of Molecular Mechanisms of Disease, University of Zürich, Zürich, Switzerland
18. Department of Orthopedics and Trauma, Medical University of Graz, Graz, Austria.
19. University Hospital of Zürich, Division of Surgical Research, Zürich, Switzerland

*Corresponding authors

One sentence summary

Intestinal IgA responses that recognize all rapidly-evolvable O-antigen variants of a *Salmonella* Typhimurium strain can drive evolutionary trade-offs for the pathogen.

Abstract

Secretory antibody responses (Immunoglobulin A, IgA) against repetitive bacterial surface glycans, such as O-antigens, can protect against intestinal pathogenic bacteria. However, vaccines that rely predominantly on secretory IgA for protection against non-Typhoidal salmonellosis often fail. Here we demonstrate that a major contributor to this failure is rapid immune escape, due to strong selective pressure exerted by high-avidity intestinal IgA. Interestingly, we found that IgA-escape initially occurs via a predictable narrow spectrum of *Salmonella* O-antigen variants that are fitness-neutral in naïve hosts. This could be attributed both to phase-variation, and to loss-of-function mutations in O-antigen-modifying enzymes. Via a vaccination regimen that simultaneously induced IgA against all observed O-antigen variants, rapid bacterial evolution could be switched from a hindrance into an advantage. Here, IgA generated a selective pressure resulting in fixation of mutations causing loss of polymerized O-antigen. When transmitted into naive hosts, these short O-antigen variants display compromised fitness and virulence, i.e. IgA-mediated pressure generates an evolutionary trade-off. Rational induction of IgA specificities that set “evolutionary traps” could reduce virulent enteropathogen reservoirs, even when sterilizing immunity cannot be achieved. This may become a powerful tool in the management of increasingly drug-resistant enteropathogenic bacteria.

Main text

While Typhoid fever-causing *Salmonella* strains can be targeted by either glycoconjugate or live-attenuated vaccines(1, 2), similar approaches have so far failed to generate a licensed vaccine against non-Typhoidal salmonellosis (NTS) in humans(3). Decades of excellent research into live-attenuated vaccines in the mouse model of typhoid fever and invasive NTS have demonstrated protection with complex underlying mechanisms including Immunoglobulin A (IgA (4–6)), T-cell mediated immunity(7, 8), mouse strain-dependent mechanisms(6), and immune-independent niche competition in the gut lumen and tissues(9, 10). However, the ability of attenuated NTS strains to grow rapidly in the gut lumen(11) is associated with prolonged intestinal shedding which may contribute to the poor safety profile described in human vaccine studies(12). In contrast, inactivated oral vaccines and glycoconjugate vaccines have a good safety profile, and can be applied in high-risk groups such as infants, pregnant women and people with immunodeficiencies(13–16). Notably, in the murine streptomycin model of NTS, inactivated oral vaccines protected predominantly via induction of high-avidity O-antigen-specific secretory IgA (17, 18). However, inactivated vaccines are typically associated with weak protection(18, 19). Here we reveal that rapid IgA-driven within-host evolution of NTS strains in the gut lumen is both a contributor and a possible solution to the poor performance of inactivated *S.Tm* vaccines.

O-Antigen, the long repetitive glycan portion of S-form lipopolysaccharide(20) (LPS), thickly carpets the surface of *Salmonella enterica* subspecies *enterica* serovar Typhimurium (*S.Tm*) (**Fig. S1**) in the gut lumen. These glycans are sufficiently long to shield non-protruding outer membrane proteins (e.g. most membrane channels(21–23)) from antibody binding(17). Therefore high-affinity intestinal IgA against O-antigen, induced by vaccination or infection(9, 24, 25), is a dominant mechanism driving clumping by enchained growth and agglutination(18). As clumped bacteria are unable to approach the gut wall, this phenomenon provides protection from disease(18, 26, 27).

We initially set out to investigate why IgA-mediated protection fails in non-Typhoidal salmonellosis. Conventional “specific opportunistic pathogen-free” (SOPF; harboring a complex microbiota, 16S amplicon analysis available in (28)) mice were vaccinated with a high-dose peracetic acid inactivated oral *S.Tm* vaccine (PA-*S.Tm*). This vaccine is prepared from wild-type *S.Tm* SL1344 and we have previously demonstrated that it protects the host predominantly via high-avidity O-antigen-binding IgA(18). Four weeks post-vaccination, these mice were antibiotic-treated to generate an open niche in the large intestine, and were subsequently infected with wild-type *S.Tm* SL1344. Vaccinated mice sporadically developed disease, involving both intestinal inflammation (quantified via fecal lipocalin 2, **Fig. 1A**) and tissue invasion (mesenteric lymph node colony forming units, CFU), **Fig. 1B**). Strikingly, disease did not correlate

with IgA titres specific for the wild-type vaccination strain, i.e. occurred despite robust high-titre vaccine-specific secretory IgA induction (**Fig. 1C**).

As the IgA response was robust, with higher titres than those observed with live-attenuated vaccines (**Fig. S2**), we investigated the phenotype of *S.Tm* clones after growth in the gut lumen of infected mice. Notably in the streptomycin mouse model of NTS, protection is independent of intestinal colonization, i.e. up to 48h post-infection the gut luminal *S.Tm* population size is similar in both vaccinated protected and vaccinated inflamed mice, with around 10^9 CFU per gram feces (18). When intestinal IgA from protected or inflamed vaccinated mice was titred against *S.Tm* clones reisolated from the feces of these mice, a very clear picture emerged. Clones isolated from the feces of protected mice were well-recognised by IgA from both groups, but IgA titres were almost undetectable against *S.Tm* clones from inflamed mice (**Fig. 1D**). This suggested the importance of another phenomenon driven by IgA: the presence of IgA exerts a strong selective pressure against *S.Tm* producing cognate antigens on its surface(18). Combined with the large population size and fast luminal growth of gut luminal pathogen cells(18), these are ideal conditions for rapid evolution of surface structures that are not bound by vaccine-induced IgA.

In order to identify changes in surface antigenicity of *S.Tm*, we phenotypically and genetically characterized the *S.Tm* clones from "vaccinated but inflamed" mice. Based on our earlier observations that protection critically depends on the O-antigen (18, 29), we focused on the O-antigen structure. The *S.Tm* O-antigen is a polymer of -mannose- α -(1 \rightarrow 4)-rhamnose- α -(1 \rightarrow 3)-galactose- α -(1 \rightarrow 2) with an acetylated α -(1 \rightarrow 3)-linked abequose at the mannose (**Fig. 1E**). WT *S.Tm* strains react strongly to O:12-0-typing antibodies (recognizing the triose backbone, Fig. S3A and B), O:5-typing antisera (recognizing the acetylated abequose) and O:4-typing antisera (recognizing the non-acetylated abequose, present due to chemical deacetylation during growth and non-stoichiometric acetylation(30)). Further, *S.Tm* has multiple options for rapidly generating O-antigen variants. *S.Tm* strain SL1344 can lose the O:5 modification, generating an O:4-only phenotype (i.e. from an O-antigen with acetylated abequose, to one with no O-acetylated abequose) by loss of function mutations in *oafA*, the abequose acetyl transferase (31). It can further shift between O:12-0 (wild-type) and O:12-2 (α -(1 \rightarrow 4) glucosylated) serotypes by methylation-dependent expression of a glucosyl transferase operon STM0557-0559 i.e. by phase variation (32, 33). This operon encodes the machinery to add glucose via an α -(1 \rightarrow 4) linkage to the backbone galactose(32). Note that *S.Tm* strain SL1344 lacks a second common operon required for linking glucose via an α -(1 \rightarrow 6) linkage to the backbone galactose, generating the O:1 serotype. These and other known variants would need to be taken into account for more diverse strains. It should be noted that both O-acetylation and backbone-glucosylation represent major changes in the hydrophobicity or steric properties of the O-antigen repeat unit, which when extensively polymerized into full-length O-antigen will have major consequences for binding of IgA raised against a different O-antigen variant (34–36).

We applied multiple techniques to determine the O-antigen structure of evolved *S.Tm* clones. Flow cytometry with serotyping antibodies (**Fig. 1F**), High Resolution-Magic Angle Spinning (HR-MAS) on intact bacteria (**Fig. S4A and B**) and ¹H-NMR (30) on purified lipopolysaccharide (**Fig. S4C**) confirmed the complete loss of abequeose O-acetylation (O:4[5] to O:4) and non-stoichiometric gain of α -(1→4)-linked glucosylation of galactose (O:12-0 to O:12-2) in clones from vaccinated but inflamed mice.

Live-attenuated vaccine strains of *S.Tm* colonize the intestine for more than 40 days in the mouse NTS model(9), i.e. sufficiently long for within-host evolution of the vaccine strain to occur. This suggested that one contributor to superior protection offered by live-attenuated vaccines could be the production of additional antibody specificities targeting evolving O-antigen variants. Correspondingly, after day 18 of colonization, when high-avidity IgA is first present in the intestine, we also observed spontaneous emergence of O:4-producing and O:12-2 producing vaccine clones, dependent on the presence of Rag1 and IgA (**Fig. S5**). Therefore, IgA-dependent selective pressures for O-antigen switching can be generated both by inactivated oral vaccines (**Fig. 1**) and by immunity arising naturally during colonization with live-attenuated strains (**Fig. S5**).

We then explored the underlying genetic mechanisms responsible for altered O-antigen structure in the evolved clones. We first determined the stability of the observed O-antigen phenotypes, i.e. whether we would see reversion during cultivation. *In vitro* serial passages of evolved clones over 5 days revealed that the switch from O:4[5] to O:4 was a stable, unimodal phenotype (**Fig. 1F and S6A**). Sequencing of O:4[5]-negative evolved clones, observed to emerge spontaneously in 9 of 29 mice vaccinated with an O:4[5]-targeting vaccine (Table S4) revealed a common 7 base-pair contraction of a tandem repeat within the *oafA* open reading frame, generating a frame-shift and loss of function (**Fig. 2A and B**). Targeted deletion of *oafA* (*S.Tm* ^{Δ oafA}) produced an identical phenotype to the 7 bp deletion (**Fig. 2B**). The same mutation was detected in 83 of 210 deposited genomes of various *Salmonella* serovars in the NCBI databank (**Fig. S7A**)(37)). As there are only two copies of the 7 base-pair motif in the wild-type ORF, the deletion of one 7 base-pair stretch is unlikely to be reversed(38) (**Fig. 2A, Fig. S7A**). Intriguingly, deposited sequences also indicate variable numbers of 9bp repeats in the promoter region of *oafA* (**Fig. S7B**), suggesting a second possible site of microsatellite instability in this gene. *oafA* also displayed strong evidence for selection-driven inactivation in a recent analysis of genomes of more than 100000 natural *Salmonella* isolates (39).

We next assessed the stability of O:12-0 to O:12-2 switching, and its underlying genetic mechanism. In contrast to O:4[5], the loss of O:12-0 staining was reversible during 3 rounds of serial *ex vivo* passage and both wild-type and evolved clones generated a bimodal staining pattern, consistent with phase variation (**Fig. 1F and S6A and B, Supplementary movies A and B**, clones referred to henceforth as O:12^{Bimodal}). In line with known epigenetic regulation of the *gtrABC* operon expression(32), re-sequencing

of the O:12^{Bimodal} strains revealed no consistent mutational pattern, although point mutations were observed across the genomes (Table S3). Instead, a semi-quantitative full-genome methylation analysis supported that evolved O:12^{Bimodal} *S.Tm* clones form mixed populations based on DNA methylation. Populations of evolved clones with up to 80% loss of reactivity with an O12-0-binding monoclonal antibody, presented a high proportion of chromosomes with a methylation pattern typical of the promoter of *gtrABC* in the ON state(32, 40, 41) and a minor population in the OFF state (**Fig. 2C and D**): a situation which is reversed in the ancestral strain. Targeted deletion of *gtrC* (*S.Tm* ^{$\Delta gtrC$}), the O:12-2 serotype-specific glucosyl transferase of the *gtrABC* operon, abolished the ability of *S.Tm* SL1344 to switch to an O:12-bimodal phenotype, even under strong *in vivo* selection (**Fig. S8**). Mathematical modeling of O:12-0/O:12-2 population sizes for fixed switching rates (supplementary methods, **Fig. S6C-E**), and comparison of flow cytometry and a *lacZ* transcriptional fusion, suggests that *in vivo* selection of O:12-2-producing clones by IgA is sufficient to explain their relative proportion in the O:12^{Bimodal} population without needing to infer any change in the switching rate (**Fig. S6**).

Therefore, selective pressure in vaccinated mice, driven by O-antigen-targeting IgA, drives the rapid emergence of *S.Tm* clones with altered O-antigen structures generated either by mutations or phase-variation. In order to quantify how strongly vaccine-induced IgA can select for O-antigen variants, we designed competition experiments using isogenic mutant pairs carrying targeted deletions in *oafA* and/or *gtrC*. This allowed us to study the selective pressure for emergence of each O-antigen variant in isolation.

We first quantified selection for the genetic switch from an **O:4[5]** to an **O:4** serotype. Competitions between *S.Tm* ^{$\Delta oafA \Delta gtrC$} (**O:4**, O:12-locked) and *S.Tm* ^{$\Delta gtrC$} (**O:4[5]**, O:12-locked) were carried out in mice vaccinated against either *S.Tm* ^{$\Delta oafA \Delta gtrC$} (**O:4**) or *S.Tm* ^{$\Delta gtrC$} (**O:4[5]**). IgA responses were strongly biased to recognition of the corresponding O:5 or O:4 *S.Tm* O-antigen epitopes and mediated a substantial selective advantage of expressing the alternative O-antigen variant (up to 10⁷-fold by day 4, **Fig. 3A-C**). The magnitude of the selective advantage correlated tightly with the magnitude of the specific IgA response against the reactive strain (**Fig. 3B-C**). Deletion of *oafA* was fitness-neutral in naïve hosts during 4 days of infection (**Fig. 3A**). These observations were repeated with identical results in Balb/c mice (**Fig. S9**). Further, the selective advantage of *S.Tm* ^{$\Delta gtrC$} over *S.Tm* ^{$\Delta oafA \Delta gtrC$} could also be observed in mice vaccinated with an O:4 variant of a commonly-used live-attenuated strain (*S.Tm* ^{$\Delta aroA \Delta oafA \Delta gtrC$} , **Fig. S10**). However, this was not observed in mice vaccinated with the standard live-attenuated O:4[5] strain, *S.Tm* ^{$\Delta aroA \Delta gtrC$} , that can undergo within-host evolution to the O:4 variant and therefore can prime immunity against both O:5 and O:4 epitopes (**Fig. S10**). Specific IgA can therefore act as a strong evolutionary pressure selecting for mutations in genes encoding O-antigen-modifying enzymes.

We next quantified the selective advantage of phase-variation between **O:12-0** and **O:12-2** using strains with an *oafA*-mutant background (i.e. O:4-locked, to prevent uncontrolled O:[4]5 to O:4 mutational changes). Mice were mock-vaccinated or vaccinated against *S.Tm* ^{$\Delta oafA \Delta gtrC$} (**O:12-locked**). Competitive infections were then carried out between *S.Tm* ^{$\Delta oafA$} (**O:12-phase-variable**) and *S.Tm* ^{$\Delta oafA \Delta gtrC$} (**O:12-locked**) strains. In line with published data(32, 42), we observe a very mild fitness benefit of O:12 phase variation in naïve mice. In contrast, phase-variation was a major benefit to *S.Tm* in a subset of vaccinated animals (**Fig. 3D**). On closer examination, precisely these animals showed a strong bias of their IgA response towards recognition of O:12-0 only (**Fig. 3E**). In animals where no out-competition was observed, the IgA response equally recognized strains producing O-antigens with either the O:12-0 or the O:12-2 O-antigen (**Fig. 3E**). This is likely explained by the stochastic nature of antibody generation towards different epitopes of the O-antigen repeat. Logically, phase-variation is beneficial whenever one phase variant is poorly bound by IgA. Correspondingly, O:12-phase variation, vaccine escape and inflammation were largely observed in mice where IgA bound poorly to the O:12-2 variant (**Fig. 3F and G**). The mechanistic basis of this selective advantage could be confirmed by complementation of the *gtrC* gene in trans (**Fig. S11**). It is interesting to note that *gtrABC* operons are often found in temperate phage(33, 43), suggesting that the ability of *S.Tm* to quickly evade IgA mediated immunity may be further promoted by co-option of phage-encoded fitness factors (morons(44)).

Our results led to the conclusion that IgA escapers, i.e. *S.Tm* mutants or phase variants only weakly recognized by vaccine-induced IgA, are strongly selected for and dominate the luminal *S.Tm* population within 1-3 days of infection in vaccinated mice. A good correlation was observed between dominance of IgA escapers and initiation of intestinal inflammation, as quantified by fecal Lipocalin 2 (LCN2, **Fig. 3G, S12**). Thus, both mutation and epigenetic switching processes shape the O-antigen structure of *S.Tm* SL1344 and can increase the pathogen's fitness in the intestine of mice immune to specific O-antigen variants. Based on a published analysis of natural *Salmonella* isolates (39), these changes arise randomly in the natural pathogen populations and appear to be slowly selected against by minor fitness reductions at evolutionary time scales. Correspondingly, they inflict negligible loss of pathogen fitness in naive hosts within the timescales of our experiments (**Fig. 3A and D**). A major disadvantage of inactivated vaccines over live vaccines is, therefore, their inability to follow this within-host evolution trajectory in order to induce broader IgA responses.

From these observations we hypothesized that a vaccine combining all four observed O-antigen variants (“Evolutionary Trap” vaccine, abbreviated as PA-*S.Tm*^{ET}; generated by mixing vaccines containing the **O:4[5],12** *S.Tm* ^{$\Delta gtrC$} , **O:4,12** *S.Tm* ^{$\Delta oafA \Delta gtrC$} , **O:4,12-2** *S.Tm* ^{$\Delta oafA$} *pgtrABC*, and **O:4[5],12-2** *S.Tm* *pgtrABC* strains) should generate enhanced disease protection against *S.Tm* SL1344 by cutting off the observed O-antigen escape pathways. Interestingly although this vaccine induced a broader antibody response (**Fig. 4A**), we did not reach significance for improved protection as

determined by intestinal inflammatory markers, and colonization of mesenteric lymph nodes and spleen (Kruskall-Wallis test on mLN CFU at d3 p.i., **Fig. S13**). This is likely due to the low-frequency of IgA-escape in this cohort of PA-S.Tm^{WT}-vaccinated C57BL/6 mice, as we do observe a robust improvement in protection in Balb/c mice where the challenge inoculum was a 1:1 mixture of O:4[5] and O:4-producing *S.Tm* variants (**Fig. S9**). More striking was that PA-S.Tm^{ET} vaccination selected for another class of O-antigen variant: mutations generating a single-repeat O-antigen(45). These can be identified by weak binding to typing antisera (**Fig. 4B**) and by gel electrophoresis of purified LPS (**Fig. 4C**). Sequencing of evolved clones (Table S4) revealed a common large deletion encompassing the *wzyB* gene (also termed *rfc*), encoding the O-antigen polymerase(45) (**Fig. 4D**, **Fig. S14** also reported in some "non-typable" *S.Tm* isolates from broilers(45)). This deletion is mediated by site-specific recombination between direct repeats flanking the *wzyB* locus, which renders the locus unstable. Short O-antigen-producing clones were detected in 10 of 13 PA-S.Tm^{ET} vaccinated mice by phenotypic characterization (anti-O5^{dim} flow cytometry staining), and *wzyB* deletion was confirmed resequencing of n=5 short-O-antigen clones from two different mice (**Table S4**). Of note, this is not an exhaustive analysis and we cannot currently exclude that other mutations could also give rise to short O-antigen mutants. However, we did not observe mutations in *wbaP*(45) (complete loss of O-antigen), *wzz*, *fepE* (46), or *opvAB*(47) (dysregulated O-antigen length) in any of the sequenced clones. Intestinal IgA from PA-S.Tm^{ΔoafA} vaccinated mice showed higher titres against the long O-antigen than the single-repeat O-antigen (**Fig. 4E**). This weaker binding to the very short O-antigen-producing strains is consistent with lower O-antigen abundance or loss of avidity (**Fig. 4B**, **Fig. S3C**).

Of note, we have previously published that IgA responses against the surface of rough *Salmonella* are identically induced by vaccination with either rough or wild-type *Salmonella* oral vaccines(17). Correspondingly, including the *wzyB* mutant into our PA-S.Tm^{ET} mix does not further improve IgA titres specific for *S.Tm*^{ΔoafA ΔgrC ΔwzyB} (**Fig. S13**), and does not improve the protective power of PA-S.Tm^{ET} (**Fig. S13**). Rather we suggest that the single-repeat O-antigen represents a fitness optimum for *S.Tm* SL1344 in orally vaccinated mice, where the decreased abundance of O-antigen repeats, and/or loss of binding by IgA specificities requiring more than one repeat, provides an advantage.

Single infections revealed that, in comparison to isogenic wild type counterparts, *wzyB*-deficient mutants (synthetic or evolved) are significantly less efficient at colonizing the gut of streptomycin pretreated naïve mice (**Fig. 4F**), disseminating systemically (**Fig. 4G**) and triggering inflammation (**Fig. 4H**). This attenuation can be attributed to compromised outer membrane integrity(48) and also manifests as an increased sensitivity to complement-mediated lysis, bile acids and weak detergents (**Fig S15**).

To verify that IgA can select for short-O-antigen-producing strains, we then tested whether IgA-mediated selection could drive outgrowth of synthetic *wzyB* deletion

mutants. Competitions between *S.Tm* ^{$\Delta oafA \Delta grC$} (O:4,12-locked, **long O-antigen**) and *S.Tm* ^{$\Delta oafA \Delta grC \Delta wzyB$} (O:4,12-locked, **single repeat O-antigen**) mutants in the intestine of vaccinated and mock-vaccinated or antibody-deficient mice revealed a substantial fitness loss due to the *wzyB* deletion in naïve animals, as observed in earlier studies(45, 49) (**Fig. 4I**). However, in the gut of vaccinated mice, the fitness cost of decreased outer-membrane integrity in *wzyB* mutants was clearly outweighed by the benefit of avoiding O-antigen specific IgA binding (**Fig. 4I**). Vaccinated IgA^{-/-} mice were indistinguishable from naïve mice in these experiments, i.e. IgA and not any other effect of the vaccine was responsible for the phenotype. PA-*S.Tm*^{ET}-elicited IgA can therefore select for *S.Tm* SL1344 mutants with a fitness cost in naïve hosts.

To demonstrate that vaccine-induced IgA, and not further genetic change in *S.Tm*, drives this out-competition, we carried out fecal transfer experiments into naïve, streptomycin-treated recipients. Full fecal pellets from PA-*S.Tm*^{ET} vaccinated mice that had been infected for 4 days with the short/long O-antigen mixture were delivered to streptomycin-treated naïve hosts. *S.Tm* ^{$\Delta oafA \Delta grC \Delta wzyB$} (short O-antigen) dominated the population in the donor feces. However, on transfer to the naïve environment the *wzyB* mutant was rapidly out-competed by the *S.Tm* ^{$\Delta oafA \Delta grC$} (full length O-antigen) (**Fig. 4J-L**). Thus, outgrowth in vaccinated mice is not due to compensatory mutations in the *wzyB* mutants, but to antibody-mediated selection.

IgA-mediated evolutionary traps work on the premise that *S.Tm* experiences two levels of selection: within-host and between-host. By dramatically altering the within-host selective landscape, we fix mutations that are detrimental under between-host selective pressures. Between-host selection, for example between farm animals, includes a period of exposure to environmental stresses, as well as transit through the hostile upper gastrointestinal tract, and invasion into a limited intestinal niche. Both published data (50), and our own analyses of susceptibility of short-O-antigen strains to membrane stress (**Fig. S15**) indicate that these strains are less likely to survive in the environment, or in the presence of high concentrations of bile acids. As the streptomycin mouse model involves a very stable intestinal niche for *S.Tm*, requiring only a single virulent *S.Tm* to be transferred in order to generate full-blown disease in the naïve host(51), we instead investigated the effect of *wzyB* mutations on *S.Tm* infection and transmission in the western diet model(28). Fecal pellets were recovered from mice pre-treated with streptomycin and infected with *S.Tm* with either a complete or single-repeat O-antigen. Recipient mice fed western diet for 24h prior to exposure received a complete fecal pellet from an infected donor and *S.Tm* counts in feces, mesenteric lymph nodes and spleen were tracked over 4 days of infection. Exposure of western diet-fed mice to fecal pellets from streptomycin-pretreated mice only resulted in disease when the donor mouse was infected with *S.Tm*^{WT} (**Fig. S16**), i.e. emergence of *wzyB*-mutants could block the disease transmission chain under these conditions.

As mouse models of transmission are necessarily rather contrived, we additionally generated a mathematical model of *Salmonella* transmission in mice and scaled to the

more relevant setting of a commercial pig farm. This model is based on literature-derived parameters and quantitatively investigates the effect of two consequences of vaccination on transmission: 1) Successful vaccination decreases the duration of shedding of viable *Salmonella* from the infected donor animals(18), and 2) fixation of *wzyB* mutations increases the death/clearance rate of *Salmonella* between shedding from the infected donor and arrival in the lower gastrointestinal tract of a new host (**Fig. S15 and 16**). Both of these factors were shown to have strong effects on the predicted R_0 of a *Salmonella* outbreak where the required infectious dose is large and the period of microbiota disturbance in the recipient animals is limited (**Fig. S17**). Correspondingly, a weak effect of vaccination on transmission is expected in the streptomycin mouse model of infection, but a strong effect (sufficient to keep R_0 below 1) would be predicted on a pig farm (see supplementary methods for detailed model description).

In conclusion, high-avidity intestinal IgA targeting the bacterial surface exerts a strong negative selective pressure on *S.Tm*. Combined with rapid growth and a large population size in the gut lumen, this selects for phase-variants or fixation of mutations that alter major cell surface antigens, and therefore facilitates *S.Tm* immune escape. Via a tailored cocktail of IgA specificities, it is possible to turn this rapid immune escape into a tool to force an evolutionary trade-off, i.e. driving outgrowth of *S.Tm* mutants producing very short O-antigens. Short O-antigen-bearing mutants have a fitness disadvantage in the environment and on transmission into naive hosts(50, 52), with important implications for disease spread. While we stress that these observations have been made only with the SL1344 strain of *Salmonella* Typhimurium, the concept of tracking the evolutionary trajectories of bacterial pathogens in vaccinated animals to design IgA “evolutionary traps” should extend to more diverse strains. This concept converts the rapid within-host evolution of intestinal bacteria from a major barrier, into a major benefit for such vaccination strategies. Of note, the evolutionary trap principle should also be relevant for the design of recombinant or synthetic glycoconjugate vaccines, and even O-antigen-targeting phage therapy. While other immune mechanisms, such as cellular immunity and surface protein-targeting antibodies can clearly improve protection (7, 53), the ability of tailored IgA responses to drive O-antigen evolution in the gut lumen will be a powerful addition to the vaccination toolbox. Evolutionary trap strategies can therefore be applied in the race to contain increasingly antibiotic resistant *Enterobacteriaceae*(54) in both humans and farm animals.

References

1. R. Milligan, M. Paul, M. Richardson, A. Neuberger, Vaccines for preventing typhoid fever. *Cochrane Database Syst. Rev.* **2018** (2018), doi:10.1002/14651858.CD001261.pub4.
2. M. M. Gibani, C. Britto, A. J. Pollard, Typhoid and paratyphoid fever: A call to action. *Curr. Opin. Infect. Dis.* **31**, 440–448 (2018).
3. S. M. Tennant, C. A. MacLennan, R. Simon, L. B. Martin, M. I. Khan,

- Nontyphoidal salmonella disease: Current status of vaccine research and development. *Vaccine*. **34**, 2907–2910 (2016).
4. I. D. Iankov, D. P. Petrov, I. V. Mladenov, I. H. Haralambieva, O. K. Kaley, M. S. Balabanova, I. G. Mitov, Protective efficacy of IgA monoclonal antibodies to O and H antigens in a mouse model of intranasal challenge with *Salmonella enterica* serotype Enteritidis. *Microbes Infect.* **6**, 901–910 (2004).
 5. A. F. Richards, J. E. Doering, S. A. Lozito, J. J. Varrone, G. G. Willsey, M. Pauly, K. Whaley, L. Zeitlin, N. J. Mantis, Inhibition of invasive salmonella by orally administered iga and igg monoclonal antibodies. *PLoS Negl. Trop. Dis.* **14**, 1–23 (2020).
 6. F. Fransen, E. Zagato, E. Mazzini, B. Fosso, C. Manzari, S. El Aidy, A. Chiavelli, A. M. D’Erchia, M. K. Sethi, O. Pabst, M. Marzano, S. Moretti, L. Romani, G. Penna, G. Pesole, M. Rescigno, BALB/c and C57BL/6 Mice Differ in Polyreactive IgA Abundance, which Impacts the Generation of Antigen-Specific IgA and Microbiota Diversity. *Immunity*. **43**, 527–540 (2015).
 7. R. Ravindran, J. Foley, T. Stoklasek, L. H. Glimcher, S. J. McSorley, Expression of T-bet by CD4 T Cells Is Essential for Resistance to Salmonella Infection. *J. Immunol.* **175**, 4603–4610 (2005).
 8. M. R. Nanton, S. S. Way, M. J. Shlomchik, S. J. McSorley, Cutting Edge: B Cells Are Essential for Protective Immunity against Salmonella Independent of Antibody Secretion. *J. Immunol.* **189**, 5503–5507 (2012).
 9. K. Endt, B. Stecher, S. Chaffron, E. Slack, N. Tchitchek, A. Benecke, L. Van Maele, J.-C. J.-C. Sirard, A. J. A. J. Mueller, M. Heikenwalder, A. J. A. J. Macpherson, R. Strugnell, C. von Mering, W.-D. W.-D. Hardt, The microbiota mediates pathogen clearance from the gut lumen after non-typhoidal salmonella diarrhea. *PLoS Pathog.* **6**, e1001097 (2010).
 10. P. Kaiser, R. R. Regoes, T. Dolowschiak, S. Y. Wotzka, J. Lengefeld, E. Slack, A. J. Grant, M. Ackermann, W.-D. Hardt, Cecum lymph node dendritic cells harbor slow-growing bacteria phenotypically tolerant to antibiotic treatment. *PLoS Biol.* **12**, e1001793 (2014).
 11. C. J. Anderson, M. M. Kendall, *Salmonella enterica* serovar typhimurium strategies for host adaptation. *Front. Microbiol.* **8**, 1–16 (2017).
 12. Z. Hindle, S. N. Chatfield, J. Phillimore, M. Bentley, J. Johnson, C. A. Cosgrove, M. Ghaem-Maghami, A. Sexton, M. Khan, F. R. Brennan, P. Everest, T. Wu, D. Pickard, D. W. Holden, G. Dougan, G. E. Griffin, D. House, J. D. Santangelo, S. A. Khan, J. E. Shea, R. G. Feldman, D. J. M. Lewis, Characterization of *Salmonella enterica* derivatives harboring defined aroC and *Salmonella* pathogenicity island 2 type III secretion system (ssaV) mutations by immunization of healthy volunteers. *Infect. Immun.* **70**, 3457–67 (2002).
 13. R. López-Gigosos, P. Garcia-Forteza, M. J. Calvo, E. Reina, R. Diez-Diaz, E. Plaza, Effectiveness and economic analysis of the whole cell/recombinant B subunit (WC/rbs) inactivated oral cholera vaccine in the prevention of traveller’s diarrhoea. *BMC Infect. Dis.* **9**, 65 (2009).
 14. A. Cross, A. Artenstein, J. Que, T. Fredeking, E. Furer, J. C. Sadoff, S. J. Cryz, Safety and immunogenicity of a polyvalent *Escherichia coli* vaccine in human volunteers. *J. Infect. Dis.* **170**, 834–840 (1994).
 15. A. Huttner, C. Hatz, G. van den Dobbelen, D. Abbanat, A. Hornacek, R. Frölich, A. M. Dreyer, P. Martin, T. Davies, K. Fae, I. van den Nieuwenhof, S. Thoelen, S. de Vallière, A. Kuhn, E. Bernasconi, V. Viereck, T. Kavvadias, K.

- Kling, G. Ryu, T. Hülner, S. Gröger, D. Scheiner, C. Alaimo, S. Harbarth, J. Poolman, V. G. Fonck, Safety, immunogenicity, and preliminary clinical efficacy of a vaccine against extraintestinal pathogenic *Escherichia coli* in women with a history of recurrent urinary tract infection: a randomised, single-blind, placebo-controlled phase 1b trial. *Lancet Infect. Dis.* **0** (2017), doi:10.1016/S1473-3099(17)30108-1.
16. J. Ruiz-Aragón, S. M. Peláez, J. M. Molina-Linde, A. M. Grande-Tejada, Safety and immunogenicity of 13-valent pneumococcal conjugate vaccine in infants: A meta-analysis. *Vaccine.* **31**, 5349–5358 (2013).
 17. K. Moor, S. Y. Wotzka, A. Toska, M. Diard, S. Hapfelmeier, E. Slack, Peracetic Acid Treatment Generates Potent Inactivated Oral Vaccines from a Broad Range of Culturable Bacterial Species. *Front. Immunol.* **7** (2016), doi:10.3389/fimmu.2016.00034.
 18. K. Moor, M. Diard, M. E. Sellin, B. Felmy, S. Y. Wotzka, A. Toska, E. Bakkeren, M. Arnoldini, F. Bansept, A. D. Co, T. Völler, A. Minola, B. Fernandez-Rodriguez, G. Agatic, S. Barbieri, L. Piccoli, C. Casiraghi, D. Corti, A. Lanzavecchia, R. R. Regoes, C. Loverdo, R. Stocker, D. R. Brumley, W.-D. Hardt, E. Slack, High-avidity IgA protects the intestine by enchainning growing bacteria. *Nature.* **544**, 498–502 (2017).
 19. S. P. Pfister, O. P. Schären, L. Beldi, A. Printz, M. D. Notter, M. Mukherjee, H. Li, J. P. Limenitakis, J. P. Werren, D. Tandon, M. Cuenca, S. Hagemann, S. S. Uster, M. A. Terrazos, M. Gomez de Agüero, C. M. Schürch, F. M. Coelho, R. Curtiss, E. Slack, M. L. Balmer, S. Hapfelmeier, Uncoupling of invasive bacterial mucosal immunogenicity from pathogenicity. *Nat. Commun.* **11**, 1–18 (2020).
 20. B. Liu, Y. A. Knirel, L. Feng, A. V. Perepelov, S. N. Senchenkova, P. R. Reeves, L. Wang, Structural diversity in *Salmonella* O antigens and its genetic basis. *FEMS Microbiol. Rev.* **38**, 56–89 (2014).
 21. P. van der Ley, P. de Graaff, J. Tommassen, Shielding of *Escherichia coli* outer membrane proteins as receptors for bacteriophages and colicins by O-antigenic chains of lipopolysaccharide. *J. Bacteriol.* **168**, 449–451 (1986).
 22. P. van der Ley, O. Kuipers, J. Tommassen, B. Lugtenberg, O-antigenic chains of lipopolysaccharide prevent binding of antibody molecules to an outer membrane pore protein in Enterobacteriaceae. *Microb. Pathog.* **1**, 43–9 (1986).
 23. A. T. Bentley, P. E. Klebba, Effect of lipopolysaccharide structure on reactivity of antiporin monoclonal antibodies with the bacterial cell surface. *J. Bacteriol.* **170**, 1063–8 (1988).
 24. E. Valguarnera, M. F. Feldman, in *Methods in enzymology* (2017; <http://www.ncbi.nlm.nih.gov/pubmed/28935107>), vol. 597, pp. 285–310.
 25. E. Diago-Navarro, I. Calatayud-Baselga, D. Sun, C. Khairallah, I. Mann, A. Ulacia-Hernando, B. Sheridan, M. Shi, B. C. Fries, Antibody-Based Immunotherapy To Treat and Prevent Infection with Hypervirulent *Klebsiella pneumoniae*. *Clin. Vaccine Immunol.* **24** (2017), doi:10.1128/CVI.00456-16.
 26. O. Pabst, New concepts in the generation and functions of IgA. *Nat. Rev. Immunol.* **12**, 821–832 (2012).
 27. K. P. Gopalakrishna, B. R. Macadangdang, M. B. Rogers, J. T. Tometich, B. A. Firek, R. Baker, J. Ji, A. H. P. Burr, C. Ma, M. Good, M. J. Morowitz, T. W. Hand, Maternal IgA protects against the development of necrotizing enterocolitis in preterm infants. *Nat. Med.* (2019), doi:10.1038/s41591-019-0480-9.

28. S. Y. Wotzka, M. Kreuzer, L. Maier, M. Arnoldini, B. D. Nguyen, A. O. Brachmann, D. L. Berthold, M. Zünd, A. Hausmann, E. Bakkeren, D. Hoces, E. Gül, M. Beutler, T. Dolowschiak, M. Zimmermann, T. Fuhrer, K. Moor, U. Sauer, A. Typas, J. Piel, M. Diard, A. J. Macpherson, B. Stecher, S. Sunagawa, E. Slack, W. D. Hardt, Escherichia coli limits Salmonella Typhimurium infections after diet shifts and fat-mediated microbiota perturbation in mice. *Nat. Microbiol.* **4**, 2164–2174 (2019).
29. K. Moor, S. Y. Wotzka, A. Toska, M. Diard, S. Hapfelmeier, E. Slack, Peracetic Acid Treatment Generates Potent Inactivated Oral Vaccines from a Broad Range of Culturable Bacterial Species. *Front. Immunol.* **7**, 34 (2016).
30. K. Ilg, G. Zandomenighi, G. Rugarabamu, B. H. Meier, M. Aebi, HR-MAS NMR reveals a pH-dependent LPS alteration by de-O-acetylation at abequose in the O-antigen of Salmonella enterica serovar Typhimurium. *Carbohydr. Res.* **382**, 58–64 (2013).
31. J. M. Slauch, A. A. Lee, M. J. Mahan, J. J. Mekalanos, Molecular characterization of the oafA locus responsible for acetylation of Salmonella typhimurium O-antigen: oafA is a member of a family of integral membrane trans-acylases. *J. Bacteriol.* **178**, 5904–9 (1996).
32. S. E. Broadbent, M. R. Davies, M. W. van der Woude, Phase variation controls expression of Salmonella lipopolysaccharide modification genes by a DNA methylation-dependent mechanism. *Mol. Microbiol.* **77**, 337–53 (2010).
33. M. R. Davies, S. E. Broadbent, S. R. Harris, N. R. Thomson, M. W. van der Woude, Horizontally acquired glycosyltransferase operons drive salmonellae lipopolysaccharide diversity. *PLoS Genet.* **9**, e1003568 (2013).
34. B. W. Sigurskjold, E. Altman, D. R. Bundle, Sensitive titration microcalorimetric study of the binding of Salmonella O-antigenic oligosaccharides by a monoclonal antibody. *Eur. J. Biochem.* **197**, 239–246 (1991).
35. D. A. Brummell, V. P. Sharma, N. N. Anand, D. Bilous, G. Dubuc, J. Michniewicz, C. R. MacKenzie, J. Sadowska, B. W. Sigurskjold, B. Sinnott, Probing the combining site of an anti-carbohydrate antibody by saturation-mutagenesis: role of the heavy-chain CDR3 residues. *Biochemistry.* **32**, 1180–7 (1993).
36. M. Yang, R. Simon, A. D. MacKerell, Jr., Conformational Preference of Serogroup B Salmonella O Polysaccharide in Presence and Absence of the Monoclonal Antibody Se155-4. *J. Phys. Chem. B.* **121**, 3412–3423 (2017).
37. Y. Nakai, A. Ito, Y. Ogawa, S. D. Aribam, M. Elsheimer-Matulova, K. Shiraiwa, S. M. B. Kisaka, H. Hikono, S. Nishikawa, M. Akiba, K. Kawahara, Y. Shimoji, M. Eguchi, Determination of O:4 antigen-antibody affinity level in O:5 antigen positive and negative variants of Salmonella enterica serovar Typhimurium. *FEMS Microbiol. Lett.* **364** (2017), doi:10.1093/femsle/fnx062.
38. M. Bichara, J. Wagner, I. B. Lambert, Mechanisms of tandem repeat instability in bacteria. *Mutat. Res. Mol. Mech. Mutagen.* **598**, 144–163 (2006).
39. J. L. Cherry, Selection-Driven Gene Inactivation in Salmonella. *Genome Biol. Evol.* **12**, 18–34 (2020).
40. L. M. Bogomolnaya, C. A. Santiviago, H.-J. Yang, A. J. Baumler, H. L. Andrews-Polymenis, “Form variation” of the O12 antigen is critical for persistence of Salmonella Typhimurium in the murine intestine. *Mol. Microbiol.* **70**, 1105–19 (2008).
41. E. Kintz, C. Heiss, I. Black, N. Donohue, N. Brown, M. R. Davies, P. Azadi, S.

- Baker, P. M. Kaye, M. van der Woude, Salmonella enterica Serovar Typhi Lipopolysaccharide O-Antigen Modification Impact on Serum Resistance and Antibody Recognition. *Infect. Immun.* **85** (2017), doi:10.1128/IAI.01021-16.
42. K. D. Seed, S. M. Faruque, J. J. Mekalanos, S. B. Calderwood, F. Qadri, A. Camilli, Phase Variable O Antigen Biosynthetic Genes Control Expression of the Major Protective Antigen and Bacteriophage Receptor in *Vibrio cholerae* O1. *PLoS Pathog.* **8**, e1002917 (2012).
 43. R. J. Mostowy, K. E. Holt, Diversity-Generating Machines: Genetics of Bacterial Sugar-Coating. *Trends Microbiol.* **26**, 1008–1021 (2018).
 44. H. Brussow, C. Canchaya, W.-D. Hardt, Phages and the Evolution of Bacterial Pathogens: from Genomic Rearrangements to Lysogenic Conversion. *Microbiol. Mol. Biol. Rev.* **68**, 560–602 (2004).
 45. I. Szabo, M. Grafe, N. Kemper, E. Junker, B. Malorny, Genetic basis for loss of immuno-reactive O-chain in *Salmonella enterica* serovar Enteritidis veterinary isolates. *Vet. Microbiol.* **204**, 165–173 (2017).
 46. G. L. Murray, S. R. Attridge, R. Morona, Regulation of *Salmonella typhimurium* lipopolysaccharide O antigen chain length is required for virulence; identification of FepE as a second Wzz. *Mol. Microbiol.* **47**, 1395–1406 (2003).
 47. I. Cota, M. A. Sánchez-Romero, S. B. Hernández, M. G. Pucciarelli, F. García-Del Portillo, J. Casadesús, Epigenetic Control of *Salmonella enterica* O-Antigen Chain Length: A Tradeoff between Virulence and Bacteriophage Resistance. *PLoS Genet.* **11**, e1005667 (2015).
 48. E. R. Rojas, G. Billings, P. D. Odermatt, G. K. Auer, L. Zhu, A. Miguel, F. Chang, D. B. Weibel, J. A. Theriot, K. C. Huang, The outer membrane is an essential load-bearing element in Gram-negative bacteria. *Nature.* **559**, 617–621 (2018).
 49. G. L. Murray, S. R. Attridge, R. Morona, Altering the length of the lipopolysaccharide O antigen has an impact on the interaction of *Salmonella enterica* serovar Typhimurium with macrophages and complement. *J. Bacteriol.* **188**, 2735–9 (2006).
 50. L. V. Collins, S. Attridge, J. Hackett, Mutations at *rfc* or *pmi* attenuate *Salmonella typhimurium* virulence for mice. *Infect. Immun.* **59**, 1079–1085 (1991).
 51. P. Kaiser, M. Diard, B. Stecher, W.-D. Hardt, The streptomycin mouse model for *Salmonella* diarrhea: functional analysis of the microbiota, the pathogen's virulence factors, and the host's mucosal immune response. *Immunol. Rev.* **245**, 56–83 (2012).
 52. K. Ilg, K. Endt, B. Misselwitz, B. Stecher, M. Aebi, W. D. Hardt, O-antigen-negative *Salmonella enterica* serovar typhimurium is attenuated in intestinal colonization but elicits colitis in streptomycin-treated mice. *Infect. Immun.* **77**, 2568–2575 (2009).
 53. S. M. Baliban, M. Yang, G. Ramachandran, B. Curtis, S. Shridhar, R. S. Laufer, J. Y. Wang, J. Van Druff, E. E. Higginson, N. Hegerle, K. M. Varney, J. E. Galen, S. M. Tennant, A. Lees, A. D. MacKerell, M. M. Levine, R. Simon, Development of a glycoconjugate vaccine to prevent invasive *Salmonella Typhimurium* infections in sub-Saharan Africa. *PLoS Negl. Trop. Dis.* **11**, 1–27 (2017).
 54. WHO | Antimicrobial resistance: global report on surveillance 2014. *WHO* (2016).

55. A. Varki, R. D. Cummings, M. Aebi, N. H. Packer, P. H. Seeberger, J. D. Esko, P. Stanley, G. Hart, A. Darvill, T. Kinoshita, J. J. Prestegard, R. L. Schnaar, H. H. Freeze, J. D. Marth, C. R. Bertozzi, M. E. Etzler, M. Frank, J. F. Vliegenthart, T. Lütteke, S. Perez, E. Bolton, P. Rudd, J. Paulson, M. Kanehisa, P. Toukach, K. F. Aoki-Kinoshita, A. Dell, H. Narimatsu, W. York, N. Taniguchi, S. Kornfeld, Symbol Nomenclature for Graphical Representations of Glycans. *Glycobiology*. **25**, 1323–1324 (2015).
56. G. R. Harriman, M. Bogue, P. Rogers, M. Finegold, S. Pacheco, A. Bradley, Y. Zhang, I. N. Mbawuiké, Targeted deletion of the IgA constant region in mice leads to IgA deficiency with alterations in expression of other Ig isotypes. *J. Immunol.* **162**, 2521–9 (1999).
57. H. Gu, Y. R. Zou, K. Rajewsky, Independent control of immunoglobulin switch recombination at individual switch regions evidenced through Cre-loxP-mediated gene targeting. *Cell*. **73**, 1155–64 (1993).
58. P. Mombaerts, J. Iacomini, R. S. Johnson, K. Herrup, S. Tonegawa, V. E. Papaioannou, RAG-1-deficient mice have no mature B and T lymphocytes. *Cell*. **68**, 869–77 (1992).
59. K. A. Datsenko, B. L. Wanner, One-step inactivation of chromosomal genes in *Escherichia coli* K-12 using PCR products. *Proc. Natl. Acad. Sci.* **97**, 6640–6645 (2000).
60. N. L. Sternberg, R. Maurer, Bacteriophage-mediated generalized transduction in *Escherichia coli* and *Salmonella typhimurium*. *Methods Enzymol.* **204**, 18–43 (1991).
61. B. Stecher, S. Hapfelmeier, C. Müller, M. Kremer, T. Stallmach, W.-D. Hardt, Flagella and Chemotaxis Are Required for Efficient Induction of *Salmonella enterica* Serovar Typhimurium Colitis in Streptomycin-Pretreated Mice. *Infect. Immun.* **72**, 4138–4150 (2004).
62. A. M. Bolger, M. Lohse, B. Usadel, Trimmomatic: a flexible trimmer for Illumina sequence data. *Bioinformatics*. **30**, 2114–2120 (2014).
63. H. Li, R. Durbin, Fast and accurate short read alignment with Burrows-Wheeler transform. *Bioinformatics*. **25**, 1754–1760 (2009).
64. B. J. Walker, T. Abeel, T. Shea, M. Priest, A. Abouelliel, S. Sakthikumar, C. A. Cuomo, Q. Zeng, J. Wortman, S. K. Young, A. M. Earl, Pilon: an integrated tool for comprehensive microbial variant detection and genome assembly improvement. *PLoS One*. **9**, e112963 (2014).
65. P. Cingolani, A. Platts, L. L. Wang, M. Coon, T. Nguyen, L. Wang, S. J. Land, X. Lu, D. M. Ruden, A program for annotating and predicting the effects of single nucleotide polymorphisms, SnpEff: SNPs in the genome of *Drosophila melanogaster* strain w1118; iso-2; iso-3. *Fly (Austin)*. **6**, 80–92 (2012).
66. S. K. Hoiseth, B. A. D. Stocker, Aromatic-dependent *Salmonella typhimurium* are non-virulent and effective as live vaccines. *Nature*. **291**, 238–239 (1981).
67. M. Barthel, S. Hapfelmeier, L. Quintanilla-Martínez, M. Kremer, M. Rohde, M. Hogardt, K. Pfeffer, H. Rüssmann, W.-D. Hardt, Pretreatment of mice with streptomycin provides a *Salmonella enterica* serovar Typhimurium colitis model that allows analysis of both pathogen and host. *Infect. Immun.* **71**, 2839–58 (2003).
68. K. Moor, J. Fadlallah, A. Toska, D. Sterlin, M. L. Balmer, A. J. Macpherson, G. Gorochov, M. Larsen, E. Slack, Analysis of bacterial-surface-specific antibodies in body fluids using bacterial flow cytometry. *Nat. Protoc.* **11**, 1531–1553 (2016).

69. M. Arnoldini, I. A. Vizcarra, R. Peña-Miller, N. Stocker, M. Diard, V. Vogel, R. E. Beardmore, W.-D. Hardt, M. Ackermann, Bistable expression of virulence genes in salmonella leads to the formation of an antibiotic-tolerant subpopulation. *PLoS Biol.* **12**, e1001928 (2014).
70. S. van Vliet, A. Dal Co, A. R. Winkler, S. Spriewald, B. Stecher, M. Ackermann, Spatially Correlated Gene Expression in Bacterial Groups: The Role of Lineage History, Spatial Gradients, and Cell-Cell Interactions. *Cell Syst.* **6**, 496-507.e6 (2018).
71. O. Westphal, K. Jann, Bacterial Lipopolysaccharides Extraction with Phenol-Water and Further Applications of the Procedure. *Methods Carbohydr. Chem.* **5**, 83–91 (1965).
72. T. Steffens, K. Duda, B. Lindner, F.-J. Vorhölter, H. Bednarz, K. Niehaus, O. Holst, The lipopolysaccharide of the crop pathogen *Xanthomonas translucens* pv. *translucens*: chemical characterization and determination of signaling events in plant cells. *Glycobiology.* **27**, 264–274 (2017).
73. S. Ardisson, P. Redder, G. Russo, A. Frandi, C. Fumeaux, A. Patrignani, R. Schlapbach, L. Falquet, P. H. Viollier, Cell Cycle Constraints and Environmental Control of Local DNA Hypomethylation in α -Proteobacteria. *PLoS Genet.* **12**, e1006499 (2016).
74. H. Li, A statistical framework for SNP calling, mutation discovery, association mapping and population genetical parameter estimation from sequencing data. *Bioinformatics.* **27**, 2987–93 (2011).
75. D. W. Barnett, E. K. Garrison, A. R. Quinlan, M. P. Strömberg, G. T. Marth, BamTools: a C++ API and toolkit for analyzing and managing BAM files. *Bioinformatics.* **27**, 1691–2 (2011).
76. A. R. Quinlan, I. M. Hall, BEDTools: a flexible suite of utilities for comparing genomic features. *Bioinformatics.* **26**, 841–2 (2010).
77. P. J. Kersey, J. E. Allen, I. Armean, S. Boddu, B. J. Bolt, D. Carvalho-Silva, M. Christensen, P. Davis, L. J. Falin, C. Grabmueller, J. Humphrey, A. Kerhornou, J. Khobova, N. K. Aranganathan, N. Langridge, E. Lowy, M. D. McDowall, U. Maheswari, M. Nuhn, C. K. Ong, B. Overduin, M. Paulini, H. Pedro, E. Perry, G. Spudich, E. Tapanari, B. Walts, G. Williams, M. Tello-Ruiz, J. Stein, S. Wei, D. Ware, D. M. Bolser, K. L. Howe, E. Kulesha, D. Lawson, G. Maslen, D. M. Staines, Ensembl Genomes 2016: more genomes, more complexity. *Nucleic Acids Res.* **44**, D574–D580 (2016).
78. M. RStudio, Inc., Boston, RStudio: Integrated Development for R, (available at <https://www.rstudio.com/>).
79. R: A Language and Environment for Statistical Computing. R Foundation for Statistical Computing, (available at <https://www.r-project.org/about.html>).
80. M. I. Love, W. Huber, S. Anders, Moderated estimation of fold change and dispersion for RNA-seq data with DESeq2. *Genome Biol.* **15**, 550 (2014).
81. M. Ackermann, B. Stecher, N. E. Freed, P. Songhet, W. D. Hardt, M. Doebeli, Self-destructive cooperation mediated by phenotypic noise. *Nature.* **454**, 987–990 (2008).
82. B. F. Sansom, P. T. Gleed, The ingestion of sow's faeces by suckling piglets. *Br. J. Nutr.* **46**, 451–456 (1981).
83. L. Montagne, G. Boundry, C. Favier, I. Le Huerou-Luron, J. P. Lallès, B. Sève, Main intestinal markers associated with the changes in gut architecture and function in piglets after weaning. *Br. J. Nutr.* **97**, 45–57 (2007).
84. H. Yamashita, A. Taoka, T. Uchihashi, T. Asano, T. Ando, Y. Fukumori,

- Single-Molecule Imaging on Living Bacterial Cell Surface by High-Speed AFM. *J. Mol. Biol.* **422**, 300–309 (2012).
85. M. Hoffmann, T. Muruvanda, M. W. Allard, J. Korlach, R. J. Roberts, R. Timme, J. Payne, P. F. McDermott, P. Evans, J. Meng, E. W. Brown, S. Zhao, Complete Genome Sequence of a Multidrug-Resistant *Salmonella enterica* Serovar Typhimurium var. 5- Strain Isolated from Chicken Breast. *Genome Announc.* **1** (2013), doi:10.1128/genomeA.01068-13.
86. C. Silva, E. Calva, J. L. Puente, M. B. Zaidi, P. Vinuesa, Complete Genome Sequence of *Salmonella enterica* Serovar Typhimurium Strain SO2 (Sequence Type 302) Isolated from an Asymptomatic Child in Mexico. *Genome Announc.* **4** (2016), doi:10.1128/genomeA.00253-16.
87. Y. Hong, M. A. Liu, P. R. Reeves, Progress in Our Understanding of Wzx Flippase for Translocation of Bacterial Membrane Lipid-Linked Oligosaccharide. *J. Bacteriol.* **200**, e00154-17 (2018).

Acknowledgements

OH acknowledges Heiko Käbner for recording NMR spectra, Regina Engel for GLC-MS, and Katharina Jakob and Sylvia Düpow for technical support. We want to thank Magdalena Schneider, Christine Kiessling, Elisabeth Schultheiss, Rosa-Maria Vesco and Clarisse Straub for the DNA extraction, library preparations and sequencing of the bacterial isolates. MD acknowledges Delphine Cornillet and the group of Prof. Dirk Bumann for serum resistance measurements.

ES, WDH and MD acknowledge Prof. Markus Aebi and Dr. Joshua Cherry for their helpful discussion and insight, as well as members of the Hardt, Slack, and Diard groups for their comments.

Funding

MD is supported by a SNF professorship (PP00PP_176954). ES acknowledges the support of the Swiss National Science Foundation (40B2-0_180953, 310030_185128, NCCR Microbiomes) and Gebert Rüt Microbials (GR073_17). MD and ES acknowledge the Botnar Center for Child Health Multi-Investigator Project 2020. BMS acknowledges the support of R01 AI041239/AI/NIAID NIH HHS/United States. WDH acknowledges support by grants from the Swiss National Science Foundation (SNF; 310030B-173338, 310030_192567, NCCR Microbiomes), the Promedica Foundation, Chur, the Gebert Rüt foundation (Displacing ESBL, with AE) and the Helmut Horten Foundation. EB is supported by a Boehringer Ingelheim Fonds PhD fellowship. BM acknowledges support by the Swiss National Science Foundation (200020_159707).

Author contributions

MD, WDH and ES designed the project and wrote the paper. MD and ES designed and carried out experiments. MvdW, BHM, RM contributed to experimental design / data interpretation. EB, DH, VL FB, KSM, AH, JA, PV, LV, DW, FB, AE, GZ, OH, MA, CL carried out analyses shown in Fig1-4 and S1-S17. ND produced strains 891 and 931. LP, AL and BMS generated novel antibody reagents. All authors critically reviewed the manuscript.

Conflict of Interest

The authors declare that Evolutionary Trap Vaccines are covered by European patent application EP19177251.

Data and materials availability

All data and materials are in the manuscript or will be provided on request to the corresponding authors.

List of Supplementary Materials:

- Materials and Methods
- Supplementary Figures S1-11
- Supplementary Table S1-5
- Supplementary Movies 1 and 2
- Supplementary .fcs files used to generate presented data

Figure legends

Figure 1: IgA-escape by O-antigen modification: **A-C:** Naïve (n=22) or PA-*S.Tm*-vaccinated (Vaccinated, n=23) SOPF mice were streptomycin-pretreated, infected (10^5 *S.Tm*^{wt} Colony forming units (CFU) per os) and analyzed 18 h later. **A.** Fecal Lipocalin 2 (LCN2) to quantify intestinal inflammation, **B.** Pathogen loads (CFU) in mesenteric lymph nodes (MLN), **C.** Intestinal IgA titres against *S.Tm*^{wt} determined by flow cytometry, for vaccinated mice with LCN2 values below (open symbols, protected) and above (filled symbols, inflamed) 100ng/g. $p=0.61$ by Mann Whitney U test. **D.** SOPF mice vaccinated and infected as in **A-C** for 3 days. Titre of intestinal lavage IgA from “inflamed vaccinated” mouse (red borders) or a “protected vaccinated” mouse (black borders) against *S.Tm* clones re-isolated from the feces of the “inflamed vaccinated” mouse (red filled circles) or “protected vaccinated” mouse (open circles) at day 3 post-infection. 2-way ANOVA with Bonferroni post-tests on log-normalized data. Clones and lavages from n=1 mouse, representative of 9 “vaccinated but inflamed” and 13 “vaccinated protected” mice, summarized in Table S4. **E.** Schematic of the O-antigen of *S.Tm* (O:4[5],12), and its common variants (O:4,12_2), coloured to correspond to the "Symbol Nomenclature for Glycans". **F.** Overnight cultures of the indicated *S.Tm* strains and evolved clones arising during infections with *S.Tm*^{wt} were stained with anti-O:5 and anti-O:12-0 antibodies, followed by fluorescent secondary reagents. Representative flow cytometry analyses of the different O-antigen types, and the "Symbol Nomenclature for Graphical Representations of Glycans"(55) representation of the O-antigen repeat structure present on *S.Tm* in each quadrant of the flow cytometry plots.

Figure 2: Genetic and epigenetic changes underlie escape: **A.** Alignment of the *oafA* sequence from wild type (SL1344_RS11465) and an example O:5-negative evolved clone showing the 7bp contraction leading to premature stop codon (all four re-sequenced O:5-negative strains showed the same deletion). **B.** Flow cytometry staining of *S.Tm*, *S.Tm* ^{Δ oafA}, and two evolved clones differing in O:5 status with anti-O:5 typing sera. **C.** Methylation status of the *gtrABC* promoter region in *S.Tm*, and three O:12^{Bimodal} evolved clones determined by REC-seq. Heat-scale for normalized read-counts, schematic diagram of promoter methylation associated with ON and OFF phenotypes, and normalized methylation read counts for the indicated strains **D.** Binding of an O-12-specific monoclonal antibody to *S.Tm* and O:12^{Bimodal} evolved clones, determined by bacterial flow cytometry.

Figure 3: O-antigen modification confers a selective advantage in the presence of vaccine-induced IgA: **A-C.** Naïve (closed circles, n=5), PA-*S.Tm* ^{Δ gtrC}-vaccinated (O:4[5]-vaccinated, open circles, n=5) and PA-*S.Tm* ^{Δ gtrC Δ oafA}-vaccinated (O:4-vaccinated, open squares, n=5) SOPF mice were streptomycin-pretreated, infected (10^5 CFU, 1:1 ratio of *S.Tm* ^{Δ gtrC} and *S.Tm* ^{Δ gtrC Δ oafA} per os). **A.** Competitive index (CFU *S.Tm* ^{Δ gtrC}/CFU *S.Tm* ^{Δ gtrC Δ oafA}) in feces at the indicated time-points. 2-way ANOVA

with Bonferroni post-tests on log-normalized values, compared to naive mice. * $p < 0.05$, ** $p < 0.01$, *** $p < 0.001$, **** $p < 0.0001$. **B** and **C**. Correlation of the competitive index with the O:4[5]-specific (**B**) and O:4-specific (**C**) intestinal IgA titre, r^2 values of the linear regression of log-normalized values. Open circles: Intestinal IgA from O:4[5]-vaccinated mice, Open squares: Intestinal IgA from O:4-vaccinated mice. Lines indicate the best fit with 95% confidence interval **D-G**. Naive (closed circles, $n=5$) or PA-*S.Tm* ^{Δ oafA Δ gtrC}-vaccinated (O:4/O:12-vaccinated, open circles and red circles, $n=10$) SOPF mice were streptomycin-pretreated and infected (10^5 CFU, 1:1 ratio of *S.Tm* ^{Δ oafA} (O:12-2 switching) and *S.Tm* ^{Δ oafA Δ gtrC} (O:12-locked) per os). **D**. Competitive index (CFU *S.Tm* ^{Δ oafA Δ gtrC} / CFU *S.Tm* ^{Δ oafA}) in feces at the indicated time-points. Red circles indicate vaccinated mice with a competitive index below 10^{-2} and are used to identify these animals in panels **D-G**. Effect of vaccination is not significant by 2-way ANOVA considering vaccination over time. **E**. Correlation of the competitive index on day 4 with the intestinal IgA titre against an O:12-2-locked *S.Tm* *pgtrABC* variant (linear regression of log-normalized values, lines indicate the best fit with 95% confidence interval). **F**. Enrichment cultures of the fecal *S.Tm* ^{Δ oafA} population at day 4 were stained for O:12/O:4 and the fraction of O:12-negative *S.Tm* quantified by flow cytometry. **G**. Intestinal inflammation quantified by measuring Fecal Lipocalin 2 (LCN2). *Note the lines joining the points are to allow individual animals to be tracked over time, and do not imply assumptions about what occurs between the measured time-points.*

Figure 4: Vaccines combining fitness-neutral glycan variants set an evolutionary trap for *S.Tm*, selecting for strains with a single-repeat O-antigen: A and B. *S.Tm* clones re-isolated from the feces of SOPF mice vaccinated with PBS only, PA-*S.Tm* ^{Δ gtrC} ($n=7$) or PA-*S.Tm*^{ET} (combined PA-*S.Tm* ^{Δ gtrC}, PA-*S.Tm* ^{Δ oafA Δ gtrC}, PA-*S.Tm* *pgtrABC*, and PA-*S.Tm* ^{Δ oafA} *pgtrABC*, $n=8$). **A**. Intestinal IgA titre determined by bacterial flow cytometry against *S.Tm* ^{Δ gtrC} (O:4[5],12), *S.Tm* ^{Δ oafA Δ gtrC} (O:4,12), *S.Tm* ^{Δ gtrC} *pgtrABC* (O:4[5], 12-2) and *S.Tm* ^{Δ oafA Δ gtrC} *pgtrABC* (O:4,12-2). **B**. Fraction of clones with weak anti-sera staining, as determined by flow cytometry screening, indicative of O-antigen shortening. One point represents one mouse. **C**. Silver-stained gel of LPS from representative control and evolved *S.Tm* strains from control and PA-*S.Tm*^{ET} vaccinated mice, showing short LPS in clones isolated from 2 different vaccinated PA-*S.Tm*^{ET} mice. **D**. Resequencing of strains with short O-antigen revealed a large genomic deletion between inverted repeats, comprising the *wzyB* gene (O-antigen polymerase) ($n=5$ clones, isolated from 2 different mice). **E**. Intestinal IgA titre from PA-*S.Tm* ^{Δ oafA Δ gtrC}-vaccinated SOPF mice specific for *S.Tm* ^{Δ oafA Δ gtrC} (long O-antigen) and *S.Tm* ^{Δ oafA Δ gtrC Δ wzyB} (short O-antigen). **F, G, H**, Single 24h infections in streptomycin pretreated naïve mice ($n=14$, short O-antigen, $n=9$ long O-antigen). Evolved and synthetic *wzyB* mutants have reduced ability to colonize the gut (**F**, CFU/g feces) and to spread systemically (**G**, CFU per mesenteric lymph node (MLN)). This translates into diminished propensity to trigger intestinal inflammation in comparison to *wzyB* wild type strains (**H**, fecal Lipocalin 2 (LCN2)). **I**. Mock-vaccinated wild type (C57BL/6; $n=10$), PA-*S.Tm* ^{Δ oafA Δ gtrC}-vaccinated JH^{-/-} mice (JH^{-/-}; $n=6$), PA-*S.Tm* ^{Δ oafA}

$\Delta gtrC$ -vaccinated wild type (C57BL/6, n=16) and PA-STm $\Delta oafA \Delta gtrC$ -vaccinated JH $^{+/-}$ littermate controls (JH $^{+/-}$, n=5 mice were streptomycin pre-treated and infected with 10^5 CFU of a 1:1 ratio *S.Tm* $\Delta oafA \Delta gtrC \Delta wzyB$ and *S.Tm* $\Delta oafA \Delta gtrC$ i.e. serotype-locked, short and long O-antigen-producing strains. Competitive index of *S.Tm* in feces on the indicated days. **J**. Feces from the indicated mice (grey-filled circles) from panel **I** were transferred into streptomycin-pretreated naive mice (one fecal pellet per mouse, n=5) and competitive index in feces calculated at day 2 post-infection. **I**: 2-way ANOVA and **J**: Paired t-test results are shown. **K** and **L**. Fecal Lipocalin 2 (LCN2) corresponding to panels **I** and **J** respectively. **A**, **I**, **K**. 2-way ANOVA on log-Normalized data. Bonferroni post-test statistics are shown. In panel **I**, competitive index in vaccinated mice is significantly higher than 1 at all time-points by Wilcoxon signed rank tests. **D**, **F**, **G**, **H**: Mann-Whitney U 2-tailed tests.

Supplementary Materials

Materials and methods:

Ethics statement

All animal experiments were approved by the legal authorities (licenses 223/2010, 222/2013 and 193/2016; Kantonales Veterinäramt Zürich, Switzerland) and performed according to the legal and ethical requirements.

Mice

Unless otherwise stated, all experiments used specific opportunistic pathogen-free (SOPF) C57BL/6 mice. 129S1/SvImJ, IgA^{-/-} (56), Balb/c, JH^{-/-} (57), Rag1^{-/-} (58) (all C57BL/6 background) and 129.SJL mice, were re-derived into a specific opportunistic pathogen-free (SOPF) foster colony to normalize the microbiota and bred under full barrier conditions in individually ventilated cages in the ETH Phenomics center (EPIC, RCHCI), ETH Zürich and were fed a standard chow diet. Low complex microbiota (LCM) mice (C57BL/6) are ex-germfree mice, which were colonized with a naturally diversified Altered Schaedler flora in 2007(9) and were bred in individually ventilated cages or flexible-film isolators at this facility, and received identical diet. Vaccinations were started between 5 and 6 weeks of age, and males and females were randomized between groups to obtain identical ratios wherever possible. As strong phenotypes were expected, we adhered to standard practice of analysing at least 5 mice per group. Western diet without fibre (BioServ, S3282; 60% kcal fat; irradiated; per mass: 36% fat, 20.5% protein, 35.7% carbohydrates, 0% fibre) was fed ad libitum where indicated. Researchers were not blinded to group allocation.

Strains and plasmids

All strains and plasmids used in this study are listed **Table S1**.

For cultivation of bacteria, we used lysogeny broth (LB) containing appropriate antibiotics (i.e., 50 µg/ml streptomycin (AppliChem); 6 µg/ml chloramphenicol (AppliChem); 50 µg/ml kanamycin (AppliChem); 100 µg/ml ampicillin (AppliChem)). Dilutions were prepared in Phosphate Buffer Saline (PBS, Difco)

In-frame deletion mutants (e.g. *gtrC::cat*) were performed by λ red recombination as described in(59). When needed, antibiotic resistance cassettes were removed using the temperature-inducible FLP recombinase encoded on pCP20(59). Mutations coupled with antibiotic resistance cassettes were transferred into the relevant genetic background by generalized transduction with bacteriophage P22 HT105/1 *int-201*(60). Primers used for genetic manipulations and verifications of the constructions are listed **Table S2**. Deletions of *gtrA* and *gtrC* originated from in-frame deletions made in *S.Tm* 14028S, kind gifts from Prof. Michael McClelland (University of California, Irvine), and were transduced into the SB300 genetic background.

The *gtrABC* operon (STM0557-0559) was cloned into the pSC101 derivative plasmid pM965(61) for constitutive expression. The operon *gtrABC* was amplified from the chromosome of SB300 using the Phusion Polymerase (ThermoFisher Scientific) and

primers listed **Table S2**. The PCR product and pM965 were digested with PstI-HF and EcoRV-HF (NEB) before kit purification (SV Gel and PCR Clean up System, Promega) and ligation in presence of T4 ligase (NEB) following manufacturer recommendations. The ligation product was transferred by electro-transformation in competent SB300 cells.

Targeted sequencing

Targeted re-sequencing by the Sanger method (Microsynth AG) was performed on kit purified PCR products (Promega) from chromosomal DNA or expression vector templates using pre-mixed sequencing primers listed **Table S2**.

Whole-genome re-sequencing of O:12^{Bimodal} isolates

The genomes of *S.Tm* and evolved derivatives were fully sequenced by the Miseq system (2x300bp reads, Illumina, San Diego, CA) operated at the Functional Genomic Center in Zürich. The sequence of *S.Tm* SL1344 (NC_016810.1) was used as reference. Quality check, reads trimming, alignments, SNPs and indels calling were performed using the bioinformatics software CLC Workbench (Qiagen).

Whole-genome sequencing of *S.Tm* isolates from "Evolutionary Trap" vaccinated mice and variant calling.

Nextera XT libraries were prepared for each of the samples. The barcoded libraries were pooled into equimolar concentrations following manufacturer's guidelines (Illumina, San Diego, CA) using the Mid-Output Kit for paired-end sequencing (2×150 bp) on an Illumina NextSeq500 sequencing platform. Raw data (mean virtual coverage 361x) was demultiplexed and subsequently clipped of adapters using Trimmomatic v0.38 with default parameters(62). Quality control passing read-pairs were aligned against reference genome/plasmids (Accession numbers: NC_016810.1, NC_017718.1, NC_017719.1, NC_017720.1) with bwa v0.7.17(63). Genomic variant were called using Pilon v1.23(64). with the following parameters: (i) minimum coverage 10x; (ii) minimum quality score = 20; (iii) minimum read mapping quality = 10. SnpEff v4.3 was used to annotate variants according to NCBI and predict their effect on genes(65).

PA-STm vaccinations

Peracetic acid killed vaccines were produced as previously described(17). Briefly, bacteria were grown overnight to late stationary phase, harvested by centrifugation and re-suspended to a density of 10⁹-10¹⁰ per ml in sterile PBS. Peracetic acid (Sigma-Aldrich) was added to a final concentration of 0.4% v/v. The suspension was mixed thoroughly and incubated for 60 min at room temperature. Bacteria were washed once in 40 ml of sterile 10x PBS and subsequently three times in 50 ml sterile 1x PBS. The final pellet was re-suspended to yield a density of 10¹¹ particles per ml in sterile PBS (determined by OD600) and stored at 4°C for up to three weeks. As a quality control, each batch of vaccine was tested before use by inoculating 100 µl of the killed vaccine (one vaccine dose) into 300 ml LB and incubating over night at 37 °C with aeration.

Vaccine lots were released for use only when a negative enrichment culture had been confirmed. For all vaccination, 10^{10} particles, suspended in 100 μ l PBS were delivered by oral gavage, once weekly for 4 weeks. Where multiple strains were combined, the total number of vaccine particles remained constant, and was roughly equally divided between the constituent strains. Unless otherwise stated, PA-STm vaccinated mice were challenged orally on d28 after the first vaccination.

Vaccination by attenuated strains of non-typhoidal *Salmonella*

6-week-old C57Bl/6 or 129 Sv/Ev mice were orally pretreated 24 h before infection with 25 mg streptomycin. *AgtrC* and *ΔoafA ΔgtrC* derivatives of the *ΔaroA* mutant (**Table S1**, (66)) were cultivated overnight separately in LB containing streptomycin. Subcultures were prepared before infections by diluting overnight cultures 1:20 in fresh LB without antibiotics and incubation for 4 h at 37°C. The cells were washed in PBS and 50 μ l of resuspended pellets were used to infect mice *per os* (5×10^7 CFU).

Feces were sampled at day 1, 9 and 42 post-infection, homogenized in 1 ml PBS by bead beating (3mm steel ball, 25 Hz for 1 minute in a TissueLyser (Qiagen)), and *S.Tm* strains were enumerated by selective plating on MacConkey agar supplemented with streptomycin. Samples for lipocalin-2 measurements were kept homogenized in PBS at -20 °C.

Non-typhoidal *Salmonella* challenge infections

Infections were carried out as described(67). Unless otherwise stated (i.e. where western diet was used for microbiota disruption), in order to allow reproducible gut colonization, 8-12 week-old C57Bl/6 or 129 Sv/Ev mice, naïve or vaccinated, were orally pretreated 24 h before infection with 25 mg streptomycin or 20 mg of ampicillin. Strains were cultivated overnight separately in LB containing the appropriate antibiotics. Subcultures were prepared before infections by diluting overnight cultures 1:20 in fresh LB without antibiotics and incubation for 4 h at 37°C. The cells were washed in PBS and 50 μ l of resuspended pellets were used to infect mice *per os* (5×10^5 CFU). Competitions were performed by inoculating 1:1 mixtures of each competitor strain.

Feces were sampled daily, homogenized in 1 ml PBS by bead beating (3 mm steel ball, 25 Hz for 1 min in a TissueLyser (Qiagen)), and *S.Tm* strains were enumerated by selective plating on MacConkey agar supplemented with the relevant antibiotics. Samples for lipocalin-2 measurements were kept homogenized in PBS at -20°C. At endpoint, intestinal lavages were harvested by flushing the ileum content with 2 ml of PBS using a cannula. The mesenteric lymph nodes, were collected, homogenized in PBS Tergitol 0.05% v/v at 25 Hz for 2 min, and bacteria were enumerated by selective plating.

Competitive indexes were calculated as the ratio of relative population sizes of competitors at a given time point, normalized for the ratio in the inoculum.

Where western diet was used to disrupt the microbiota, mice were switched from standard chow to western diet (BioServ, S3282) 24 h prior to infection and were maintained on western diet throughout the infection.

Non-typhoidal *Salmonella* transmission

Donor mice were vaccinated with PA-*S.Tm* ^{Δ oafA Δ gtrC} once per week for 5 weeks, streptomycin pretreated (25 mg streptomycin *per os*), and gavaged 24 h later with 10⁵ CFU of a 1:1 mixture of *S. Tm* ^{Δ oafA Δ gtrCwzyB::cat} (Cm^R) and *S. Tm* ^{Δ oafA Δ gtrC^{Kan}} (Kan^R). On day 4 post infection, the donor mice were euthanized, organs were harvested, and fecal pellets were collected, weighed and homogenized in 1 ml of PBS. The re-suspended feces (centrifuged for 10 s to discard large debris) were immediately used to gavage (as a 50 μ l volume containing the bacteria from one fecal pellet) recipient naïve mice (pretreated with 25 mg streptomycin 24 hours before infection). Recipient mice were euthanized and organs were collected on day 2 post transmission. In both donor and recipient mice, fecal pellets were collected daily and selective plating was used to enumerate *Salmonella* and determine the relative proportions (and consequently the competitive index) of both competing bacterial strains.

Quantification of fecal Lipocalin2

Fecal pellets collected at the indicated time-points were homogenized in PBS by bead-beating at 25 Hz, 1 min. Large particles were sedimented by centrifugation at 300 g, 1 min. The resulting supernatant was then analysed in serial dilution using the mouse Lipocalin2 ELISA duoset (R&D) according to the manufacturer's instructions.

Analysis of IgA-coating, and O:5/O:12-0 expression on *S.Tm* in cecal content

Fresh cecal content or feces was re-suspended in sterile PBS by bead-beating at 25 Hz, 1 min (previously demonstrated to disrupt IgA cross-linked clumps(18)). An aliquot estimated to contain not more than 10⁶ *S.Tm* was directly stained with a monoclonal human IgG-anti-O:12-0 (STA5(18)) and biotin-conjugated anti-mouse IgA clone RMA-1 (Biolegend), and/or Rabbit-anti-*Salmonella* O:5 (Difco). After washing, secondary reagents Alex647-anti-human IgG (Jackson ImmunoResearch), Pacific Blue-conjugated streptavidin (Molecular Probes), Phycoerythrin-conjugated streptavidin (Molecular Probes) and/or Brilliant violet 421-anti-Rabbit IgG (Biolegend) were added. After a final washing step, samples were analysed on a BD LSRII flow cytometer, or a Beckman Coulter Cytoflex S, with settings adapted for optimal detection of bacterial-sized particles. The median fluorescence intensity of IgA staining on *S.Tm* was determined by "gating" on bacterial sized particles and calculating the appropriate median fluorescence corresponding to O:12-0 or O:5 staining FlowJo (Treestar, USA). Gates used to calculate the % of "ON" and "OFF" cells were calculated by gating on samples with known ON or OFF phenotypes.

Analysis of specific antibody titers by bacterial flow cytometry

Specific antibody titers in mouse intestinal washes were measured by flow cytometry as described(18, 68). Briefly, intestinal washes were collected by flushing the small intestine with 5 ml PBS, centrifuged at 16000 g for 30 min and aliquots of the supernatants were stored at -20°C until analysis. Bacterial targets (antigen against which antibodies are to be titered) were grown to late stationary phase or the required

OD, then gently pelleted for 2 min at 3000 g. The pellet was washed with sterile-filtered 1% BSA/PBS before re-suspending at a density of approximately 10^7 bacteria per ml. After thawing, intestinal washes were centrifuged again at 16000 g for 10 min. Supernatants were used to perform serial dilutions. 25 μ l of the dilutions were incubated with 25 μ l bacterial suspension at 4°C for 1 h. Bacteria were washed twice with 200 μ l 1% BSA/PBS before resuspending in 25 μ l 1% BSA/PBS containing monoclonal FITC-anti-mouse IgA (BD Pharmingen, 10 μ g/ml) or Brilliant violet 421-anti-IgA (BD Pharmingen). After 1 h of incubation, bacteria were washed once with 1% BSA/PBS and resuspended in 300 μ l 1% BSA/PBS for acquisition on LSRII or Beckman Coulter Cytoflex S using FSC and SSC parameters in logarithmic mode. Data were analysed using FloJo (Treestar). After gating on bacterial particles, log-median fluorescence intensities (MFI) were plotted against antibody concentrations for each sample and 4-parameter logistic curves were fitted using Prism (Graphpad, USA). Titers were calculated from these curves as the inverse of the antibody concentration giving an above-background signal.

Flow cytometry for analysis of O:5, O:4 and O:12-0 epitope abundance on *Salmonella* in cecal content, enrichment cultures and clonal cultures

1 μ l of overnight cultures, or 1 μ l of fresh feces or cecal content suspension (as above) was stained with STA5 (human recombinant monoclonal IgG2 anti-O:12(18)), Rabbit anti-*Salmonella* O:5 or Rabbit anti-*Salmonella* O:4. After incubation at 4°C for 30 min, bacteria were washed once with PBS/1% BSA and resuspended in appropriate secondary reagents (Alexa 647-anti-human IgG, Jackson ImmunoResearch, Brilliant Violet 421-anti-Rabbit IgG, Biolegend). This was incubated for 10-60 min before cells were washed and resuspended for acquisition on a BD LSRII or Beckman Coulter Cytoflex S.

Live-cell immunofluorescence

200 μ L of an overnight culture was centrifuged and resuspended in 200 μ L PBS containing 1 μ g recombinant murine IgA clone STA121-AlexaFluor568. The cells and antibodies were co-incubated for 20 min at room temperature in the dark and then washed twice in 1 mL Lysogeny broth (LB). Antibody-labeled cells were pipetted into an in-house fabricated microfluidic device(69). Cells in the microfluidic device were continuously fed *S.Tm*-conditioned LB(69) containing STA121-AlexaFluor568 (1 μ g/mL). Media was flowed through the device at a flow rate of 0.2 mL/h using syringe pumps (NE-300, NewEra PumpSystems). Cells in the microfluidic device were imaged on an automated Olympus IX81 microscope enclosed in an incubation chamber heated to 37°C. At least 10 unique positions were monitored in parallel per experiment. Phase contrast and fluorescence images were acquired every 3 min. Images were deconvoluted in MatLab(70). Videos are compressed to 7 fps, i.e. 1 s = 21 mins.

HR-MAS NMR

S. Typhimurium cells were grown overnight (~18 h) a to late stationary phase. The equivalent of 11–15 OD₆₀₀ was pelleted by centrifugation for 10 min 4 °C and 3750 g. The pellet was resuspended in 10% NaN₃ in potassium phosphate buffer (PPB; 10 mM pH 7.4) in D₂O and incubated at room temperature for at least 90 min. The cells were then washed twice with PPB and resuspended in PPB to a final concentration of 0.2 OD₆₀₀/μl in PPB containing acetone (final concentration 0.1% (v/v) as internal reference). The samples were kept on ice until the NMR measurements were performed - i.e. for between 1 and 8 h. The HR-MAS NMR spectra were recorded in two batches, as follows: *S.Tm*^{WT}, *S.Tm*^{wbaP}, *S.Tm*^{Evolved_1}, *S.Tm*^{Evolved_2} were measured on 16.12.2016, *S.Tm*^{OafA} was measured on 26.7.2017.

NMR experiments on intact cells were carried out on a Bruker Biospin AVANCE III spectrometer operating at 600 MHz ¹H Larmor frequency using a 4 mm HR-MAS Bruker probe with 50 μl restricted-volume rotors. Spectra were collected at a temperature of 27 °C and a spinning frequency of 3 kHz except for the sample of OafA (25°C, 2 kHz). The ¹H experiments were performed with a 24 ms Carr–Purcell–Meiboom–Gill (CPMG) pulse-sequence with rotor synchronous refocusing pulses every two rotor periods before acquisition of the last echo signal to remove broad lines due to solid-like material(30). The 90° pulse was set to 6.5 μs, the acquisition time was 1.36 s, the spectral width to 20 ppm. The signal of HDO was attenuated using water pre-saturation for 2 s. 400 scans were recorded in a total experimental time of about 30 minutes.

O-Antigen purification and ¹H-NMR

The LPS was isolated applying the hot phenol-water method(71), followed by dialysis against distilled water until the phenol scent was gone. Then samples were treated with DNase (1mg/100 mg LPS) plus RNase (2 mg/100 mg LPS) at 37°C for 2 h, followed by Proteinase K treatment (1 mg/100 mg LPS) at 60°C for 1 h [all enzymes from Serva, Germany]. Subsequently, samples were dialyzed again for 2 more days, then freeze dried. Such LPS samples were then hydrolyzed with 1% aqueous acetic acid (100°C, 90 min) and ultra-centrifuged for 16 h at 4°C and 150,000 g. Resulting supernatants (the O-antigens) were dissolved in water and freeze-dried. For further purification, the crude O-antigen samples were chromatographed on TSK HW-40 eluted with pyridine/acetic acid/water (10/4/1000, by vol.), then lyophilized. On these samples, 1D and 2 D (COSY, TOCSY, HSQC, HMBC) ¹H- and ¹³C-NMR spectra were recorded with a Bruker DRX Avance 700 MHz spectrometer (¹H: 700.75 MHz; ¹³C: 176.2 MHz) as described(72).

Atomic force microscopy

The indicated *S.Tm* strains were grown to late-log phase, pelleted, washed once with distilled water to remove salt. A 20 μl of bacterial solution was deposited onto freshly cleaved mica, adsorbed for 1 min and dried under a clean airstream. The surface of bacteria was probed using a Dimension FastScan Bio microscope (Bruker) with Bruker AFM cantilevers in tapping mode under ambient conditions. The microscope was

covered with an acoustic hood to minimized vibrational noise. AFM images were analyzed using the Nanoscope Analysis 1.5 software.

Methylation analysis of *S.Tm* clones

For REC-Seq (restriction enzyme cleavage–sequencing) we followed the same procedure described by Ardissonne et al, 2016(73). In brief, 1 µg of genomic DNA from each *S.Tm* was cleaved with MboI, a blocked (5'biotinylated) specific adaptor was ligated to the ends and the ligated fragments were then sheared to an average size of 150-400 bp (Fasteris SA, Geneva, CH). Illumina adaptors were then ligated to the sheared ends followed by deep-sequencing using a HiSeq Illumina sequencer, the 50 bp single end reads were quality controlled with FastQC (<http://www.bioinformatics.babraham.ac.uk/projects/fastqc/>). To remove contaminating sequences, the reads were split according to the MboI consensus motif (5'-GATC-3') considered as a barcode sequence using fastx_toolkit (http://hannonlab.cshl.edu/fastx_toolkit/) (fastx_barcode_splitter.pl --bcfile barcodelist.txt --bol --exact). A large part of the reads (60%) were rejected and 40% kept for remapping to the reference genomes with bwa mem(63) and samtools(74) to generate a sorted bam file. The bam file was further filtered to remove low mapping quality reads (keeping AS >= 45) and split by orientation (alignmentFlag 0 or 16) with bamtools(75). The reads were counted at 5' positions using Bedtools(76) (bedtools genomecov -d -5). Both orientation count files were combined into a bed file at each identified 5'-GATC-3' motif using a home-made PERL script. The MboI positions in the bed file were associated with the closest gene using Bedtools closest(76) and the gff3 file of the reference genomes(77). The final bed file was converted to an MS Excel sheet with a homemade script. The counts were loaded in RStudio 1.1.442(78) with R version 3.4.4(79) and analysed with the DESeq2 1.18.1 package(80) comparing the reference strain with the 3 evolved strains considered as replicates. The counts are analysed by genome position rather than by gene. The positions are considered significantly differentially methylated upon an adjusted p-value < 0.05. Of the 2607 GATC positions, only 4 were found significantly differentially methylated and they are all located in the promoter of the *gtrABC* operon.

The first step in the reads filtering was to remove contaminant reads missing the GATC consensus motif (MboI) at the beginning of the sequence. These contaminant reads are due to random fragmentation of the genomic DNA and not to cuts of the MboI restriction enzyme. Using fastx_barcode_splitter.pl about 60% of the reads were rejected because they did not start with GATC. The rest (40%) was analyzed further. Random DNA shearing and blunt-ended ligation of adaptors, combined with sequencing noise at the beginning of reads likely generates this high fraction of reads missing at GTAC sequence.

***gtrABC* expression analysis by blue/white screening and flow cytometry.**

About 200 colonies of *S.Tm*^{*gtrABC-lacZ*} (strain background 4/74, (32)) were grown from an overnight culture on LB agar supplemented with X-gal (0.2 mg/ml, Sigma) in order to select for *gtrABC* ON (blue) and OFF clones (white). These colonies were then

picked to start pure overnight cultures. These cultures were diluted and plated on fresh LB agar X-gal plate in order to enumerate the proportion of *gtrABC* ON and OFF siblings. The proportion of O:12/O:12-2 cells was analyzed by flow cytometry.

***In vitro* growth and competitions to determine *wzyB*-associated fitness costs**

Single or 1:1 mixed LB subcultures were diluted 1000 times in 200 μ l of media distributed in 96 well black side microplates (Costar). Where appropriate, wild type *S.Tm* carried a plasmid for constitutive expression of GFP. To measure growth and competitions in stressful conditions that specifically destabilize the outer membrane of *S.Tm*, a mixture of Tris and EDTA (Sigma) was diluted to final concentration (4 mM Tris, 0.4 mM EDTA) in LB; Sodium cholate (Sigma) and Sodium Dodecyl Sulfate (SDS) (Sigma) were used at 2% and 0.05% final concentration respectively. The lid-closed microplates were incubated at 37°C with fast and continuous shaking in a microplate reader (Synergy H4, BioTek Instruments). The optical density was measured at 600 nm and the green fluorescence using 491 nm excitation and 512 nm emission filter wavelengths every 10 minutes for 18 h. Growth in presence of SDS is causing aggregation when cell density reaches OD=0.3-0.4, therefore, it is only possible to compare the growth curves for about 250 minutes. The outcome of competitions was determined by calculating mean OD and fluorescence intensity measured during the last 100 min of incubation. OD and fluorescence values were corrected for the baseline value measured at time 0.

Serum resistance

Overnight LB cultures were washed three times in PBS, OD adjusted to 0.5 and incubated with pooled human serum obtained from Unispital Basel (3 vol of culture for 1 vol of serum) at 37°C for 1 h. Heat inactivated (56°C, 30 min) serum was used as control treatment. Surviving bacteria were enumerated by plating on non-selective LB agar plates. For this, dilutions were prepared in PBS immediately after incubation.

Modeling antigen switching between O12 and O12-2

The aim of this modeling approach is to test whether a constant switching rate between an O12 and an O12-2 antigen expression state can explain the experimentally observed bimodal populations.

To this end, we formulated a deterministic model of population dynamics of the two phenotypic states as:

$$\frac{dO_{12}}{dt} = (\mu O_{12} - s_{\rightarrow 12-2} O_{12} + s_{\rightarrow 12} O_{12-2}) * \left(1 - \frac{(O_{12} + O_{12-2})}{K} \right)$$
$$\frac{dO_{12-2}}{dt} = (\mu O_{12-2} + s_{\rightarrow 12-2} O_{12} - s_{\rightarrow 12} O_{12-2}) * \left(1 - \frac{(O_{12} + O_{12-2})}{K} \right)$$

where O_{12} and O_{12-2} denote the population sizes of the respective antigen variants, μ denotes the growth rate, which is assumed to be identical for the two variants, K the

carrying capacity, and $s_{\rightarrow 12-2}$ and $s_{\rightarrow 12}$ the respective switching rates from O_{12} to O_{12-2} and from O_{12-2} to O_{12} . Growth, as well as the antigen switching rates, are scaled with population size in a logistic way, so that all processes come to a halt when carrying capacity is reached.

We use the model to predict the composition of a population after growth in LB overnight, and therefore set the specific growth rate to $\mu = 2.05h^{-1}$, which corresponds to a doubling time of roughly 20min. The carrying capacity is set to $K = 10^9$ cells. We ran parameter scans for the switching rates $s_{\rightarrow 12}$ and $s_{\rightarrow 12-2}$, with population compositions that start either with 100% or 0% O_{12} , and measure the composition of the population after 16h of growth (**Fig. S6C**). The initial population size is set to 10^4 cells

Experimentally, we observe that when starting a culture with an O_{12} colony, after overnight growth the culture is composed of around 90% O_{12} and 10% O_{12-2} cells, whereas starting the culture with O_{12-2} cells yields around 50% O_{12} and 50% O_{12-2} cells after overnight growth (**Fig. S6B**). To explain this observation without a change in switching rates, we would need a combination of values in $s_{\rightarrow 12}$ and $s_{\rightarrow 12-2}$ that yield the correct population composition for both scenarios. In **Fig. S6D**, we plot the values of $s_{\rightarrow 12}$ and $s_{\rightarrow 12-2}$ that yield values of 10% O_{12-2} (starting with 0% O_{12-2} , green dots) and 50% O_{12-2} (starting with 100% O_{12-2} , orange dots). The point clusters intersect at $s_{\rightarrow 12} = 0.144h^{-1}$ and $s_{\rightarrow 12-2} = 0.037h^{-1}$ (as determined by a local linear regression at the intersection point).

We then used the thus determined switching rates to produce a population growth curve in a deterministic simulation, using the above equations for a cultures starting with 100% O_{12-2} , (**Fig. S6E**, Left-hand graph) and for a culture starting with 0% O_{12-2} (**Fig. S4E**, right-hand graph).

These switching rates are consistent with published values (31). Our results show that the observed phenotype distributions can be explained without a change in the rate of switching between the phenotypes.

Modeling Realistic Transmission

Section 1: Central concepts in non-Typhoidal *Salmonella* transmission

Salmonella spread in a population when contaminated matter from an infected host is ingested by other susceptible hosts, which may then develop a symptomatic *Salmonella* infection. Successful vaccination itself will affect the duration of infection and the concentration of *Salmonella* shed in the feces during the infection. The Evolutionary Trap vaccine will further affect the concentration of *S.Tm* arriving in the lower GIT of a new host, as short-O-antigen mutants have a higher loss in the environment and during transit of the intestine of the next host (**Fig. S17A**). In section 2 we consider the effect of infection duration on transmission in a host population. In section 3 we calculate the probability of successful infection from a one-time exposure. In section 4 we discuss realistic parameters. In section 5 we show the expected impact of vaccination per se and evolutionary trap-driven loss-of-fitness on *Salmonella* transmission in a host population.

Section 2: Duration of infection with non-Typhoidal *Salmonella*

If the infected host is vaccinated, then the host is protected from inflammation even if an open niche in the lower gastrointestinal tract (GIT) allows *Salmonella* colonization(18). As *Salmonella* competes poorly with the microbiota in the absence of inflammation(9), the microbiota will regrow and ultimately outcompete. Thus, the duration of *Salmonella* shedding is reduced in successfully vaccinated animals. In the limit of a large and well-mixed population, if the duration of infection is reduced k -fold, then R_0 , the average number of hosts successfully infected by one infected host at the beginning of an outbreak, is also reduced by k -fold. If the population is small or not well-mixed, such that the same host may eat contaminated matter during several distinct periods of susceptibility, then the reduction will be less than k -fold.

Section 3: The probability of infection with non-Typhoidal *Salmonella*, given a one-time exposure

3.1: Concepts

A mass m of feces, containing *Salmonella* at concentration s_d , are ingested by the recipient. The number of viable *Salmonella* ingested with this fecal material will be determined by bacterial death in the environment, prior to ingestion, and death during transit of the upper GIT of the recipient, before reaching the replicative niche in the lower GIT. We denote p the overall probability of survival for each bacterium between leaving the infected animal and arriving in the lower GIT of the recipient. We define s_0 as the initial concentration of growing *Salmonella* present in the lower-GIT of the recipient as:

$$s_0 = ms_d p/M$$

with M the mass of the contents of the lower GIT. Successful vaccination per se reduces s_d , the concentration of *Salmonella* shed by the infected donor. The short O-antigen *Salmonella* have a reduced s_d as well as a reduced p , i.e. probability to survive the period of time between shedding and arrival in a new replicative niche.

For *Salmonella* to successfully cause inflammatory disease, which is required for *Salmonella* to outcompete the microbiota and generate a large stable niche for *Salmonella* in the gut lumen, its population has to reach a certain threshold of *Salmonella* concentration T in the lower GIT(79). If the microbiota is undisturbed, *Salmonella* cannot grow and reach the threshold. In reality, the exact nature of this colonization resistance is highly complex, but for the purpose of a workable model, let us denote τ the duration of a microbiota perturbation, during which the microbiota is in a low enough concentration that the growth rate of *Salmonella* will be close to its maximal growth rate. Let us define r_s the maximal growth rate and c_s the loss rate of *Salmonella*. If *Salmonella* does not get to T before the end of τ , then the gut will remain uninflamed, the microbiota will rapidly outcompete *Salmonella* and the host animal will remain healthy. The lower the initial concentration of *Salmonella*, s_0 , the more time it takes to reach the threshold T , and thus the less likely it is that *Salmonella* can compete with regrowth of the microbiota. Let us denote t_w the time window during which transmission leads to a successful *Salmonella* infection of a recipient host under a given

set of conditions. If the recipient host is at most exposed once during τ , then a k -fold reduction in the window of possible infection t_w (for example because the short O-antigen *Salmonella* transmitted from a vaccinated host has a smaller survival probability p , leading to a shorter t_w), will also reduce R_0 by k -fold. Note that if a recipient host is ingesting contaminated matter more than once during τ , then the reduction will be less than k -fold.

In what follows, we calculate the window of possible infection, as a function of the other parameters.

3.2 Calculations

3.2.1: In the absence of inflammation, the equations for the *Salmonella* concentration $S(t)$ are given by (with K the carrying capacity, and F the effective concentration of the microbiota which competes for the same resources as *Salmonella*):

$$\frac{dS}{dt} = r_s \left(1 - \frac{F + S}{K}\right) S - c_s S$$

We assume that $T \ll K$ and that during τ , $F \ll K$, thus defining $r_{\text{eff}} = r_s - c_s$ the effective net growth rate:

$$\frac{dS}{dt} \simeq (r_s - c_s) S = r_{\text{eff}} S$$

Thus $S(t) = s_0 \exp(r_{\text{eff}} t)$.

3.2.2: Window of successful salmonella infection

t_w , the time window during which successful transmission can occur, can be defined as the time interval required (between $t = 0$ (time of start of microbiota perturbation in the recipient host) and the end of the microbiota perturbation τ) for *Salmonella* growth to increase the population concentration from s_0 to T . This translates into the following equation

$$T = s_0 \exp(r_{\text{eff}}(\tau - t_w))$$

And thus

$$t_w = \tau - \frac{1}{r_{\text{eff}}} \log\left(\frac{T}{s_0}\right)$$

4. Parameters

Duration of *Salmonella* shedding

In a vaccinated infected donor, the concentration of *Salmonella* in the lower GIT (and therefore the density of *Salmonella* shed in the feces) drops more rapidly than in naïve infected donors. *Salmonella* with a short O-antigen induce less inflammation (Fig. 4H) at 24 h post-infection, even in naïve, streptomycin-pre-treated hosts. As R_0 is roughly proportional to this duration of shedding in the population, there is a strong dependence on these observations.

Net growth rate (r_{eff}): The wild-type *Salmonella* maximum net growth rate in the gut lumen r_{eff} , is experimentally found to be around 1.3 h^{-1} (18). From competitive infections of short- and wild-type-O-antigen strains, as shown in Fig. 4 I and J, we see that the relative proportion of the short-O-antigen strain decreases steadily over the 4 days of infection. The decrease in the competitive index is of the order of $10^{0.5}$ -fold a day (Fig. 4I and J), thus we can estimate the difference in net growth rate is of the order of 0.05 h^{-1} .

Period of microbiota disturbance (τ): The duration of the period τ during which the microbiota is disturbed enough that *Salmonella* can grow at r_{eff} depends on the type of perturbation present.

- Streptomycin pretreatment (1g/kg) results in a perturbation in the order of 3 days.
- Western diet exposure in mice has a τ in the order of 12 h (49).

The threshold T above which *Salmonella* induces inflammation in mice is around $5 \cdot 10^7/\text{g}$ (79). As similar densities of *Salmonella* colonization can cause disease in pigs, we make the bold assumption that this value is similar in both species.

The initial concentration of *Salmonella* s_0 in the wild-type case with no vaccination.

Mice are naturally coprophagic. In non-Typhoidal salmonellosis, the relevant gut compartment for *Salmonella* growth is the cecum, which hold a typical mass of $M = 1 \text{ g}$ contents. A contaminated fecal pellet (mass of typically $m = 10 \text{ mg}$), which at a concentration of $c = 10^9 \text{ bacteria/g}$, with a limited death of bacteria (let's assume $p = 0.3$ for instance) will mean $s_0 = mcp/M = 3 \times 10^6/\text{g}$ *Salmonella* will be present at the start of the infection.

In swine in natural settings, while c and p will likely be of the same order of magnitude, m/M is different, and will depend strongly on the conditions. The amount of contaminated matter ingested is not well characterized, and likely highly variable. The highest level will be reached for deliberate ingestion of feces. Young piglets eat daily about 20 g of feces (80), have about 24h digestion time, and total mass of their gut content if of the order of 130 g(81), which leads to m/M 0.15, instead of the 0.01 discussed previously for mice. Thus $s_0 = 5 \times 10^7/\text{g}$ is an upper bound in piglets.

The reduction in the initial concentration of *Salmonella* due to successful vaccination or successful vaccination and dominance of short O-antigen clones in the donor, s'_0/s_0 :

To simplify this case, we focus on a transmission from the donor occurring during the first 3 days after it becomes infected. During this time, *Salmonella* loads in the gut are comparable between vaccinated and unvaccinated donor mice, and reduction in transmission will be predominantly due to loss-of-fitness of the shed *Salmonella* i.e.:

As vaccination does not change fecal mass likely to be ingested (m) or the mass of lower GIT content before infection (M), m/M will remain the same. Vaccination by

itself do not change c , at least in the first days; however for short O-antigen *Salmonella*, based on Fig. 4F, c'/c will be approximately $10^{-0.5}$, giving a lowered net growth in the recipient host. The vaccination itself is not a priori changed by the vaccination itself, however for the short-O-antigen strain, p'/p will be below 1, as this strain is more susceptible to both environmental and host-derived stress. A conservative estimate of $s_0'/s_0 = 0.1$ is reasonable, and the actual difference may be much larger, as the viability of the short O-antigen *Salmonella* may be strongly affected (Fig. S15F).

5. Results and Discussion:

In Fig. S17B, we compare the relative change in R_0 in different scenarios. We take the parameters for mice, and for swine as listed above, and vary two critical parameters (shedding duration of the infected donor, and concentration of *Salmonella* arriving in the host lower gastrointestinal tract) over a large range of values.

We simulated the effect on the relative R_0 as a function of the relative duration of active *Salmonella* shedding (i.e. the relative length of the infectious period for a vaccinated versus and a naïve donor). Fig. S17B shows, as expected, that the duration of high-density *Salmonella* shedding is an important parameter, as R_0 will scale with this parameter. This duration can be affected both by the vaccination preventing inflammation, and by the presence of short O-antigen strains that are less effective colonizers of the GIT.

Another hypothesis arising from a study of the model parameters is that s_0 , i.e. the number of viable *Salmonella* arriving in the lower GIT of a recipient host, will be lower in the case of a short-O-antigen strain, than for a wild-type O-antigen strain due to weakened resistance to environmental and host stressors. Fig. S17B (y axes) shows that the long, robust microbiota perturbation in the mouse non-Typhoidal salmonellosis (streptomycin) model, makes the effect of initial dose on R_0 very small. In contrast, in a more natural system with a shorter microbiota perturbation, this parameter has more importance (Swine model).

Significance of this model for *Salmonella* transmission

An estimate for *Salmonella* transmission, based on a Danish pig farm outbreak suggests that the R_0 in typical conditions maybe around 2 (although with a large uncertainty in the estimate). In order for disease introductions to never result in a major outbreak, R_0 needs to be below 1. Therefore, achieving and R_0'/R_0 of 0.5 or lower will generate effective protection. In this model, outbreak prevention in a pig population can be achieved by decreasing the duration of shedding of the infected animal by 50%; or by 25%, if combined with a decrease in viable *Salmonella* reaching the lower GIT of the recipient of around 100-fold. The combination of faster decay of *Salmonella* fecal concentrations in vaccinated animals, and the poorer survival in the environment and during transit through the upper GIT can therefore both contribute to effective prophylaxis in realistic settings.

5.3 Sensitivity to the parameters

As we see on Fig. S17B, R'_0/R_0 has a strong dependence on the duration of shedding, and a more moderate dependence on s'_0/s_0 . What about the other parameters? Let us use the parameters of Fig. S17B and take $s'_0/s_0=0.1$ and a 2-fold reduction of shedding duration. The main difference between the mice and swine case is the duration τ of microbiota perturbation. If the microbiota perturbation was only 6 h instead of 12 h for the swine, then R'_0/R_0 would be further reduced from 0.41 to 0.33. The dependence on r_{eff} is small. A reduction of r_{eff} by 20% decreases R'_0/R_0 from 0.41 to 0.38 in the swine case, and from 0.47 to 0.46 in the mice case. We have also assumed that the r_{eff} of the short-O-antigen *Salmonella* is 0.05 h^{-1} smaller than the wild-type *Salmonella*, but this is not the main effect, as removing this assumption increases R'_0/R_0 by only about 4 % for both the mice and the swine cases. The dependence on s_0 and the threshold T is very weak. Decreasing s_0 10-fold or increasing T 10-fold only change R'_0/R_0 from 0.41 to 0.39; and in the mouse, the dependence is even weaker, a similar change reduces R'_0/R_0 by 0.2% only.

Caveats of the model:

This is a highly simplified model and cannot begin to represent the full complexity of this system. Several critical assumptions have needed to be made: 1) that infected animals with high *Salmonella* shedding remain in the herd. Daily health checks may in fact remove actively infected animals from the herd into quarantine, decreasing this period of shedding and thus R_0 , also in the unvaccinated case. 2) we have modelled a highly uniform system with a single deterministic equation. In reality, infection spread is highly stochastic. 3) we have not explicitly modeled a time-dependence of s_0 in new recipients relative to the time of the first infection, although this will vary over time. 3) the housing situation on a typical Danish pig farm may differ significantly to conditions in pig farms around the world and the necessary reduction in R_0 required to protect these farms would require a more detailed assessment of pen sizes, exposure to fecal material, cleaning regimens, etc. 4) We assume that the interaction between short O-antigen-producing *Salmonella* and vaccination is additive and not that one effect always supersedes the other. In reality, this may be more complex, as for example the evolutionary trap vaccines should better prevent outgrowth of fitness-neutral escape mutations.

Supplementary figure legends

Fig. S1: Surface phenotype of *S.Tm* mutants: A-C. Atomic force microscopy phase images of *S.Tm*^{wt}, *S.Tm* ^{$\Delta wzyB$} (single-repeat O-antigen), and *S.Tm* ^{$\Delta wbaP$} (rough mutant - no O-antigen) at low magnification (A) and high magnification (B and C). Invaginations in the surface of *S.Tm* ^{$\Delta wbaP$} (dark colour, B) show a geometry and size consistent with outer membrane pores(84). These are already less clearly visible on the surface of *S.Tm* ^{$\Delta wzyB$} with a single-repeat O-antigen, and become very difficult to discern in *S.Tm*^{wt}. C. Fast-Fourier transform of images shown in "B" demonstrating

clear regularity on the surface of *S.Tm* ^{$\Delta wbaP$} , which is progressively lost when short and long O-antigen is present.

Fig. S2: PA-STm vaccination induces higher titres of intestinal IgA than vaccination with live-attenuated *S.Tm* ^{$\Delta sseD$} . Intestinal lavage IgA from PA-STm-vaccinated mice at d28 after the first vaccination (n=5) or *S.Tm* ^{$\Delta sseD$} -chronically infected mice at day 40 post-infection (n=9) were titred against wild-type *S.Tm* by bacterial flow cytometry. Dilution factor of lavages give IgA MFI=500 is shown. Mann Whitney U test result shown.

Fig. S3: Characterization of the specificity of STA5 and STA121 using diverse *Salmonella enterica* serovars and recombinant *S.Tm* strains. **A.** Recombinant monoclonal STA5 human IgG1 was used to surface stain overnight cultures of the indicated *Salmonella enterica* serovars. Bacterial surface binding was detected with a Dylight-633-anti human IgG secondary antibody and analysed by flow cytometry. STA5 binds to all serovars that include the O:12 epitope **B.** Overnight cultures of the indicated *S.Tm* synthetic mutants were stained with STA5 and analysed as in (A). Over-expression of *gtrABC* producing O:12-2-modified O-antigen results in loss of STA5 staining. **C.** Overnight cultures of the indicated *S.Tm* synthetic mutants were stained with STA5 and analysed as in (A), or with a recombinant murine monoclonal dimeric IgA STA121, detected with Brilliant violet 421-anti-mouse IgA. Note that STA5 binds equally well to *S.Tm* with short or long O-antigen, but STA121 cannot bind to the single-repeat O-antigen. *wzyB* mutations are therefore associated, at least, with escape from vaccine-induced antibodies with similar specificities to STA121.

Fig. S4: NMR of purified LPS from the indicated strains. **A.** Schematic diagram of expected NMR peaks for each molecular species **B.** HR-MAS ¹H-NMR spectra. Spectra show predicted peak positions, and observed spectra for C1 protons of the O-antigen sugars. **C.** ¹H NMR of purified LPS from the indicated strains. Note that non-acetylated abequose can be observed in wild-type strains due to spontaneous deacetylation at low pH in late stationary phase cultures(30). A *gtrA* mutant strain is used here to over-represent the O:12-2 O-antigen variant due to loss of regulation(40).

Fig S5: *S.Tm* O-antigen variation occurs in chronic *S.Tm* infections in an antibody-dependent manner. IgA^{-/-} and Rag1^{-/-} and heterozygote littermate controls were pre-treated with streptomycin and infected with *S.Tm* ^{$\Delta sseD$} orally. Feces were collected at the indicated time-points, enriched overnight in LB plus kanamycin, stained for O:5 and O:12-0 and analysed by flow cytometry. The fraction of the population that lost O:5 and O:12-0 antisera staining is shown over time. *Note that lines joining the points are to permit tracking of individual animals through the data set, and may not be representative of what occurs between the measured time-points.*

Fig. S6: Loss of O:12-staining is a reversible phenotype. **A.** Wild type and evolved *S.Tm* clones were picked from LB plates, cultured overnight, phenotypically characterized by O:12-0 (left panel) and O:5 staining (right panel), plated and re-picked. This process was repeated over 3 cycles with lines showing the descendants of each clone. **B.** Comparison of fractions of O:12-0-positive and O:12-0-negative bacteria (in fact O:12-2) determined by flow cytometry staining with typing sera and by blue-white colony counts using a *gtrABC-lacZ* reporter strain. **C-E.** Results of a mathematical model simulating bacterial growth and antigen switching (see supplementary methods). **C.** Switching rates from O12-0 to O12-2 and from O12-2 to O12-0 were varied computationally, and the fraction of O12-2 was plotted after 16 h of growth. Left-hand plot depicts the results of the deterministic model when starting with 100% O12-2, right-hand plot depicts the results when starting with 100% O12-0. **D.** depicts only the switching rates that comply with the experimentally observed antigen ratios after overnight growth (90% O12-0 when starting with O12-0, and 50% O12-0 when starting with O12-2). Right-hand plot is a zoomed version showing values for switching rates between $0 - 0.1 \text{ h}^{-1}$ (marked by a grey rectangle in **D**), left-hand plot. Dashed lines are linear regressions on the values in this range, and their intersection marks the switching rates used for the stochastic simulation in (**E**). **E.** Simulation results of bacterial population growth, when starting with only O12-2 (left-hand plot) or only O12-0 (right-hand plot). was kept constant in all simulations; switching rates were varied in steps of in (**C** and **D**), and kept constant at and in (**E**); the starting populations were always individuals of the indicated phenotype; carrying capacity was always 10^9 cells.

Fig S7: Mutations detected in the *oafA* gene sequence among several strains of *S.Tm* **A.** Aligned fractions of the *oafA* ORF from a natural isolate (from chicken) presenting the same 7 bp deletion detected in mutants of *S.Tm* SL1344 emerging in vaccinated mice. *S.Tm* SL1344 was used a reference(85). **B.** Aligned *oafA* promoter sequences from three natural isolates of human origin (stool or cerebrospinal fluid(86)) showing variations in the number of 9 bp direct repeats.

Fig. S8: Glucosyltransferases containing loci including *gtrABC* are required for generation of the O:12^{Biomodal} phenotype: Wild type 129Sv mice were mock-vaccinated or were vaccinated with PA-*S.Tm* ^{$\Delta oafA \Delta gtrC$} as in Fig. 1A. On d28, all mice were pre-treated with streptomycin, and infected with the indicated strain. **A.** Feces recovered at day 10 post-infection, was enriched overnight by culture in streptomycin, and stained for O:12. Fraction O:12-low *S.Tm* was determined by flow cytometry. Percentage of *S.Tm* that are O:12-negative was quantified over 10 days and is plotted in panel B.

Fig. S9: IgA-drive selective pressure and Evolutionary Trap vaccines function identically in SPF Balb/c mice. **A-C.** Naive (closed circles), PA-*S.Tm* ^{$\Delta gtrC$} -vaccinated (open circles) and PA-*S.Tm*^{ET}-vaccinated (crossed-circles) SPF Balb/c mice were streptomycin-pretreated, infected (10^5 CFU, 1:1 ratio of *S.Tm* ^{$\Delta gtrC$} and *S.Tm* ^{$\Delta gtrC \Delta oafA$} per os). Note that naïve Balb/c mice were euthanized on day 3 due to severe disease. **A.** Secretory IgA titres (intestinal lavage dilution) against O:4[5], 12-0, and an O:4, 12-0 *S.Tm*. **B.** Competitive index (CFU *S.Tm* ^{$\Delta gtrC$} /CFU *S.Tm* ^{$\Delta gtrC \Delta oafA$}) in feces at the

indicated time-points. 2-way ANOVA with Bonferroni post-tests on log-normalized values, compared to naive mice. **** $p < 0.0001$. **C** and **D**. Correlation of the competitive index with the O:4-specific (**C**) and O:4[5]-specific (**D**) intestinal IgA titre, r^2 values of the linear regression of log-normalized values. Open circles: Intestinal IgA from PA-*S.Tm* ^{Δ gtrC}-vaccinated mice, crossed circles: Intestinal IgA from PA-*S.Tm*^{ET}-vaccinated mice. Lines indicate the best fit with 95% confidence interval. **E**. CFU of *S.Tm* ^{Δ gtrC} (black symbols) and *S.Tm* ^{Δ gtrC Δ oafA} (orange symbols) per gram feces at the indicated time-points. **F** and **G**. CFU of *S.Tm* ^{Δ gtrC} (black symbols) and *S.Tm* ^{Δ gtrC Δ oafA} (orange symbols) per organ and day 4 post-infection (vaccinated) and day 3 post-infection (naïve). **H**. Fecal Lipocalin 2 as a marker of inflammation in the indicated groups. 2-way repeat-measures ANOVA on log-normalized data. *** $p < 0.001$, **** $p < 0.0001$ **I** and **J**. Correlation between fecal lipocalin 2 on d3 post-infection and O:4 and O:4[5]-specific intestinal IgA titres. r^2 values of the linear regression of log-normalized values. Lines indicate the best fit with 95% confidence interval. Note that lines joining the points are to permit tracking of individual animals through the data set, and may not be representative of what occurs between the measured time-points.

Fig. S10: “Vaccination” by chronic infection with attenuated *aroA oafA* mutants but not with *aroA* mutants drives outcompetition of *oafA*-sufficient *Salmonella* on challenge, which correlates with O:4[5]-specific antibody responses. **A-E**. For challenge, *S.Tm* ^{Δ aroA Δ gtrC}-exposed (O:4[5]-vaccinated, closed circles) and *S.Tm* ^{Δ aroA Δ gtrC Δ oafA}-exposed (O:4-vaccinated, closed squares) SOPF mice (C57BL/6, black symbols; 129 Sv/Ev, blue symbols) were ampicillin-pretreated, infected (10^7 CFU, 1:1 ratio of ampicillin-resistant *S.Tm* ^{Δ gtrC} and *S.Tm* ^{Δ gtrC Δ oafA} per os). **A**. Competitive index (CFU *S.Tm* ^{Δ gtrC}/CFU *S.Tm* ^{Δ gtrC Δ oafA}) in feces at the indicated time-points. Mean significantly different from 0, One-sample t test * $p < 0.05$, ** $p < 0.01$, *** $p < 0.001$. **B**. Fecal Lipocalin 2 (LCN2). The timeline is divided between days post-infection by attenuated *aroA* strains and days post-challenge with competing virulent strains. **C**. Vaccine strains shedding at day 1, 9 and 42 post-infection. The resident *E. coli* population eventually excluded *aroA Salmonella* mutants in the 129 Sv/Ev mice (Blue symbols) **D** and **E**. Correlation of the competitive index with the O:4[5]-specific (**D**) and O:4-specific (**E**) intestinal IgA titre, r^2 values of the linear regression of log-normalized values. Closed circles: Intestinal IgA from O:4[5]-vaccinated mice, Closed squares: Intestinal IgA from O:4-vaccinated mice. Lines indicate the best fit with 95% confidence interval

Fig S11: The Δ gtrC mutation can be complemented in trans: Mice were vaccinated and pre-treated as in **Fig. 3**. The inoculum contained a 1:1 ratio of *S.Tm* ^{Δ oafA} and *S.Tm* ^{Δ oafA Δ gtrC} *pgtrABC*. Competitive index in feces was determined by differential selective plating over 4 days post-infection.

Fig S12: Fecal lipocalin-2 measurements corresponding to Fig. 3A. Fecal Lipocalin 2 (LCN2) over days 1-4 plotted against the competitive index of infection for animals

from Fig. 3A, vaccinated either against O:5-producing *S.Tm* (A), or O:4-producing *S.Tm* (B). Symbols indicate different days post-infection as indicated in the legend.

Fig S13: PA-STm^{ET} does not significantly increase protection over a wild type vaccine at day 4 post-infection. Mice were vaccinated with vehicle only (Naïve, n=10), PA-*S.Tm*^{wt} (n=8), PA-STm^{ET} (combined PA-*S.Tm*^{ΔgtrC}, PA-*S.Tm*^{ΔoafA ΔgtrC}, PA-*S.Tm* *pgtrABC*, and PA-*S.Tm*^{ΔoafA} *pgtrABC*, n=9) or PA-STm^{ET+wzyB} (combined PA-*S.Tm*^{ΔgtrC}, PA-*S.Tm*^{ΔoafA ΔgtrC}, PA-*S.Tm* *pgtrABC*, PA-*S.Tm*^{ΔoafA} *pgtrABC* and PA-*S.Tm*^{ΔoafA ΔgtrC ΔwzyB}, n=4). On day 28 after the first vaccination, mice were streptomycin pre-treated and challenged with 10⁵ *S.Tm*^{wt} orally. Fecal Lipocalin-2 (LCN2) at day 1-3 post-infection (A) and CFU *S.Tm*^{wt} per gram feces on day 1-3 post-infection (B), CFU *S.Tm*^{wt} per mesenteric lymph node (MLN) at day 3 post-infection (C), and CFU *S.Tm*^{wt} per spleen at day 3 post-infection (D). A and B, repeat-measures ANOVA reveals no significant difference between the vaccinated groups at any time-point. C and D: Kruskal-Wallis analyses were carried out for significance. Exact p values displayed. E. IgA titres of a final experiment not included in Fig. 4A), and additionally showing the group PA-*S.Tm*^{ΔoafA ΔgtrC ΔwzyB}. 2-way ANOVA on log-normalized data. Note that lines joining the points are to permit tracking of individual animals through the data set, and may not be representative of what occurs between the measured time-points.

Fig. S14: Schematic of *S.Tm* O-antigen synthesis (based on(87))

Fig. S15: Synthetic and natural deletions of *wzyB* reduce the fitness of *S.Tm* in presence of Tris-EDTA, Chololate, SDS and serum complement. The deletion of *wzyB* does not affect the growth of *S.Tm* or *S.Tm*^{ΔoafA ΔgtrC} in LB (No stress) (A) but impairs growth in presence of Tris-EDTA (B), 2% chololate (C) and 0.05% SDS (D). Dashed lines represent the range of variations between experiments. This was in line with the outcome of competitions between *S.Tm* expressing constitutive Green Fluorescent Protein (*S.Tm*^{GFP}) and *S.Tm*^{ΔoafA ΔgtrC ΔwzyB} or a *wzyB* mutant isolated from an Evoltrap vaccinated mouse (E). The level of GFP corrected for the optical density (OD) served as readout to quantify the *S.Tm*^{GFP} population at the end of the overnight growth, in presence of *S.Tm*^{ΔoafA ΔgtrC}, *S.Tm*^{ΔoafA ΔgtrC ΔwzyB} or an evolved *S.Tm*^{ΔwzyB}, in LB with or without Tris-EDTA. Values above 1 (dashed line) indicates that relatively more GFP was detected in presence of Tris-EDTA than without, which resulted from a competitive advantage of *S.Tm*^{GFP} in presence of stress. F. The deletion of *wzyB* makes *Salmonella* sensitive to human serum complement. Values below 10⁰ (dashed line) indicates that the number of colony-forming units (CFU) detected after incubation in human serum was lower than after incubation in heat inactivated human serum.

Fig. S16: Short O-antigen *S.Tm* poorly colonizes the intestine of western diet-fed mice, and transmits poorly between animals in this non-Typhoidal salmonellosis model. A-C. SOPF C57BL/6J mice were switched onto a western diet 24 h before infection with 10⁸ *S.Tm*^{ΔoafA ΔgtrC} (long O-antigen, red diamonds, n=6) or 10⁸ *S.Tm*^{ΔoafA}

$\Delta gtrC \Delta wzyB$ (Short O-antigen, black diamonds, n=7) p.o. **A.** *S.Tm* CFU per gram feces on day 1-3 post infection. **B.** *S.Tm* CFU per mesenteric lymph node (mLN) at d 3 post-infection, **C.** *S.Tm* CFU per spleen at d3 post-infection. **A.** Repeat-measures ANOVA on log-normalized data with Bonferroni post-tests. **B and C.** Mann-Whitney U tests. **D. and E.** A donor cohort of mice were pre-treated with streptomycin and infected with either 10^5 *S.Tm* ^{$\Delta oafA \Delta gtrC$} (long O-antigen, n=6) or 10^5 *S.Tm* ^{$\Delta oafA \Delta gtrC \Delta wzyB$} (Short O-antigen, n=6) p.o. The recipient mice were placed onto western diet. At 24 h post-infection (donors), and 24 h after starting western diet feeding (recipients), fecal pellets were collected from the donors, homogenized, plated to determine the donor CFU/g feces (**D**), and then concentrated into 100 μ l. *S.Tm* from one fecal pellet was used to transmit the infection into western-diet-fed recipients. **E.** *S.Tm* CFU per gram feces in recipient mice at the indicated time-points.

Fig. S17: Mathematical model of *S.Tm* transmission in mice and in domestic pigs.

A. Schematic of the model in which a vaccinated or naïve donor transmits infection into a naïve population. A new host becomes infected by ingesting a certain mass of feces containing an original *Salmonella* density of s_d . Individual *Salmonella* shed from the donor have a probability p of arriving alive in the lower gastrointestinal tract (GIT) of the new host, generating the seeding population at density s_0 . The nature of the perturbation present in the new host will determine the duration τ during which these *Salmonella* will be able to grow. If the *Salmonella* population size reaches a threshold, T , before the microbiota recovers then inflammation is triggered, and a fulminant infection develops. If s_0 is low, or the infection event occurs too late during the microbiota perturbation, then T is not reached, and the host remains healthy (see supplementary methods for more detail). **B.** Here the equations in **A** are used to investigate the effect of a shorter infectious period and lower seeding densities (s_0), due vaccination on the relative value of R_0 (R_0'/R_0 colour scale). We explore two possible scenarios. $T = 5 \times 10^7$ CFU/g for both mice and pigs. In mice pre-treated with streptomycin, $s_0 = 3 \times 10^6$ /g and $\tau = 72$ h, in swine $s_0 = 5 \times 10^7$ /g and $\tau = 12$ h. As the R_0 for *Salmonella* spread in a standard Danish pig farm is estimated to be in the order of 2, a 50% reduction in R_0 will result in extinction of the outbreak.

Supplementary Movies A and B

Visualization of O:12 phase variation using live-cell immunofluorescence. Cells expressing GFP (green) pre-stained with fluorescently-labeled recombinant murine IgA STA121 specific for the O:12-0epitope (red) were loaded into a microfluidic chip for time-lapse microscopy. Cells were fed continuously *S.Tm*-conditioned LB containing fluorescently-labeled recombinant murine IgA STA121 specific for the O:12-0epitope. (A) Loss and (B) gain of antibody reactivity (red staining) was observed, indicative of O:12 phase variation.

Supplementary Tables

Table S1: *Salmonella* strains and genotypes

Table S2: Details of primers used in strain construction, testing and sequencing

Table S3: Details of mutations found in resequenced O12-0 or O12 bimodal evolved clones studied by REC-Seq as shown in Fig. 1F and 2C-D. Numbers indicate the position of the mutation, numbers in brackets indicates the percentage of reads were the mutation was detected.

Table S4: Details of experiments in which *Salmonella* O-antigen shifts were observed

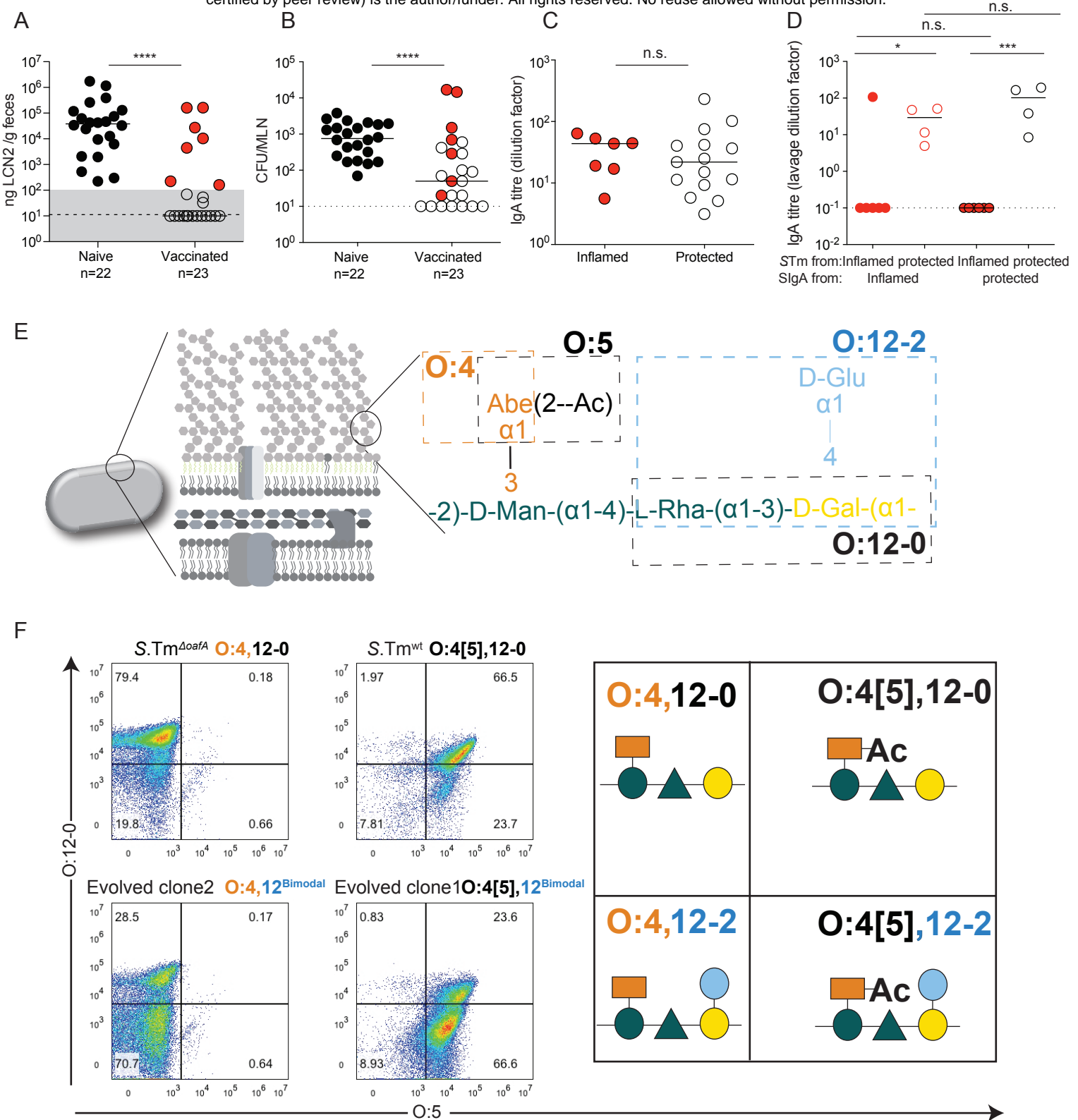


Figure 1: IgA-escape by O-antigen modification

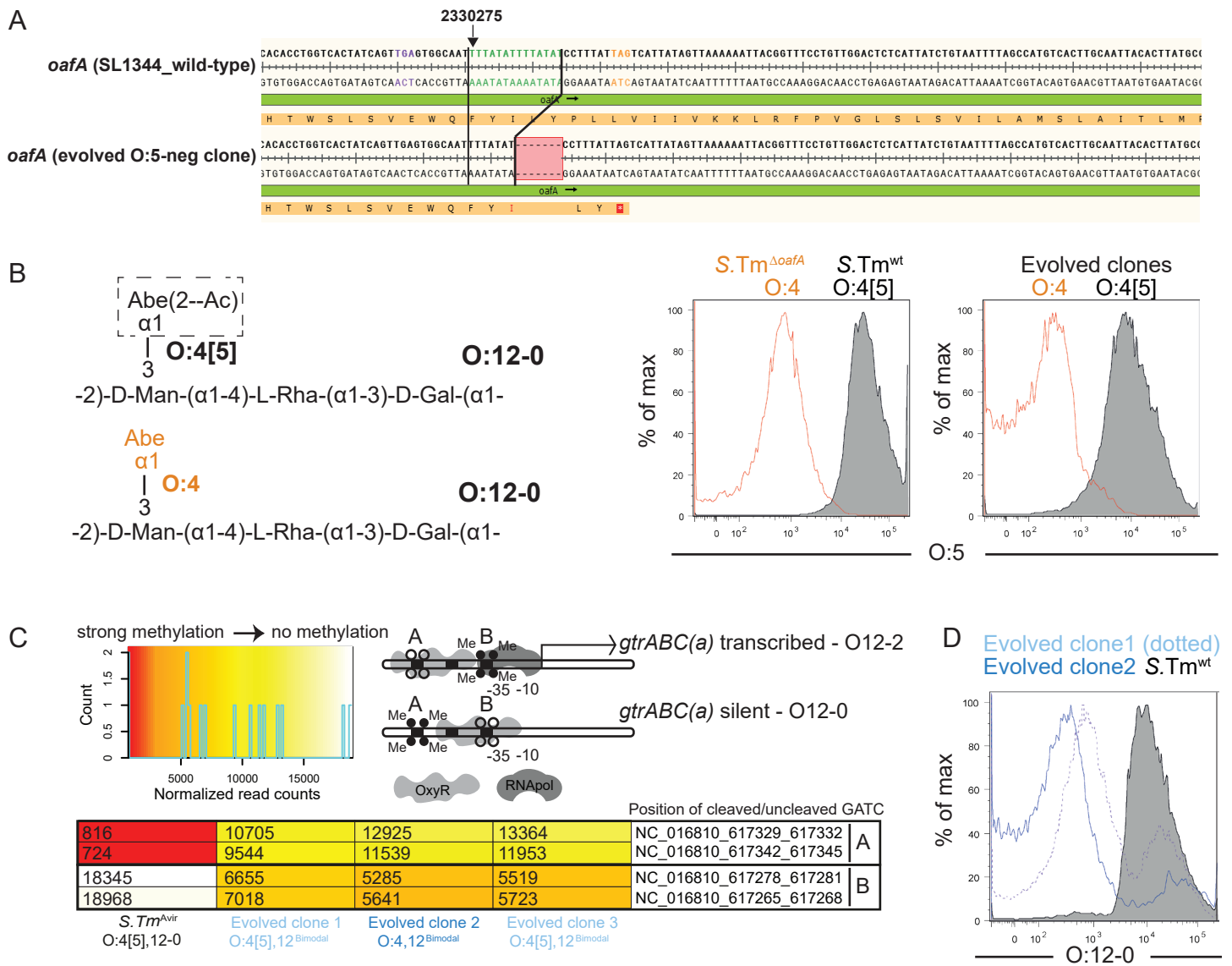


Figure 2: Genetic and epigenetic changes underlie escape

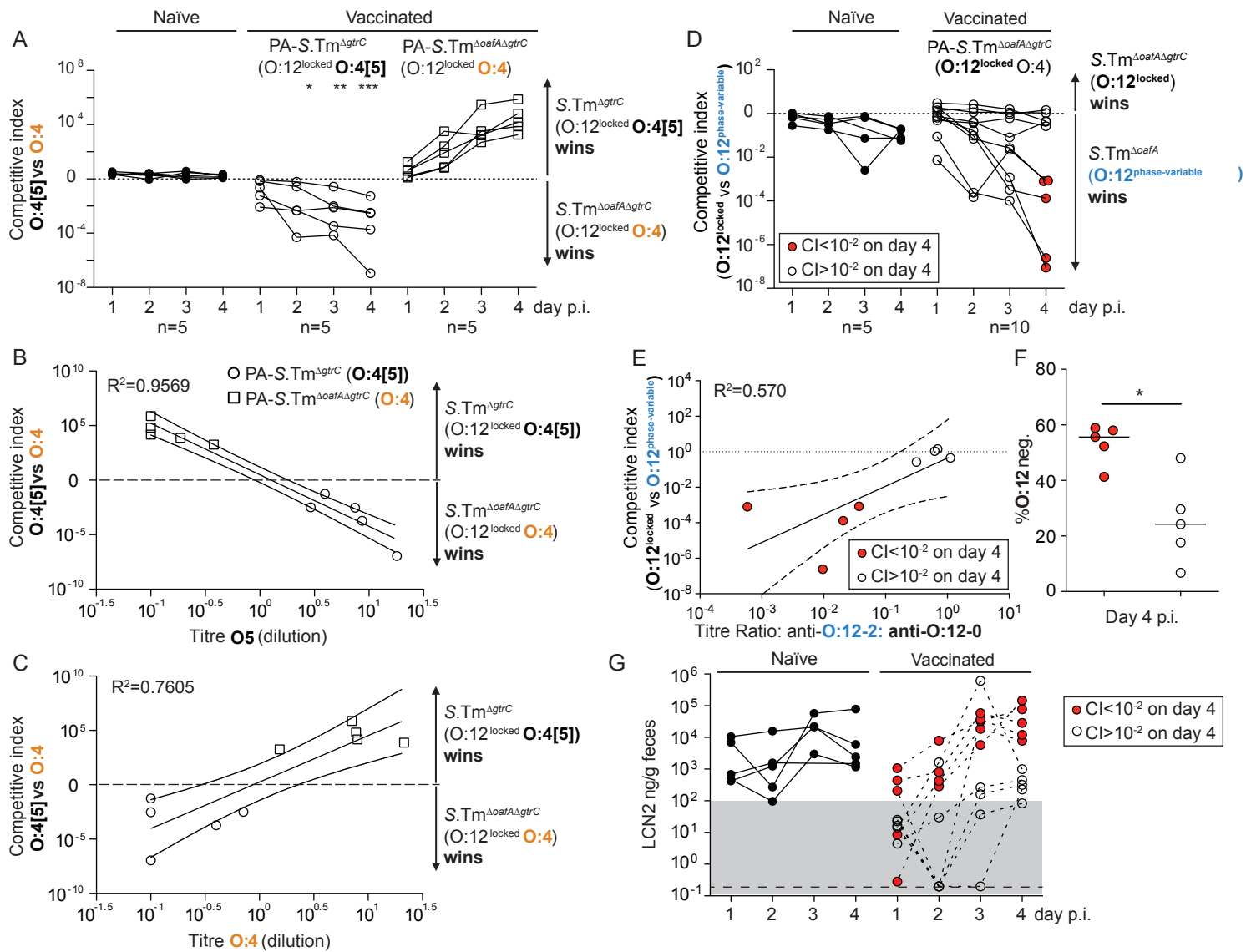


Figure 3: O-antigen modification confers a selective advantage in the presence of vaccine-induced IgA

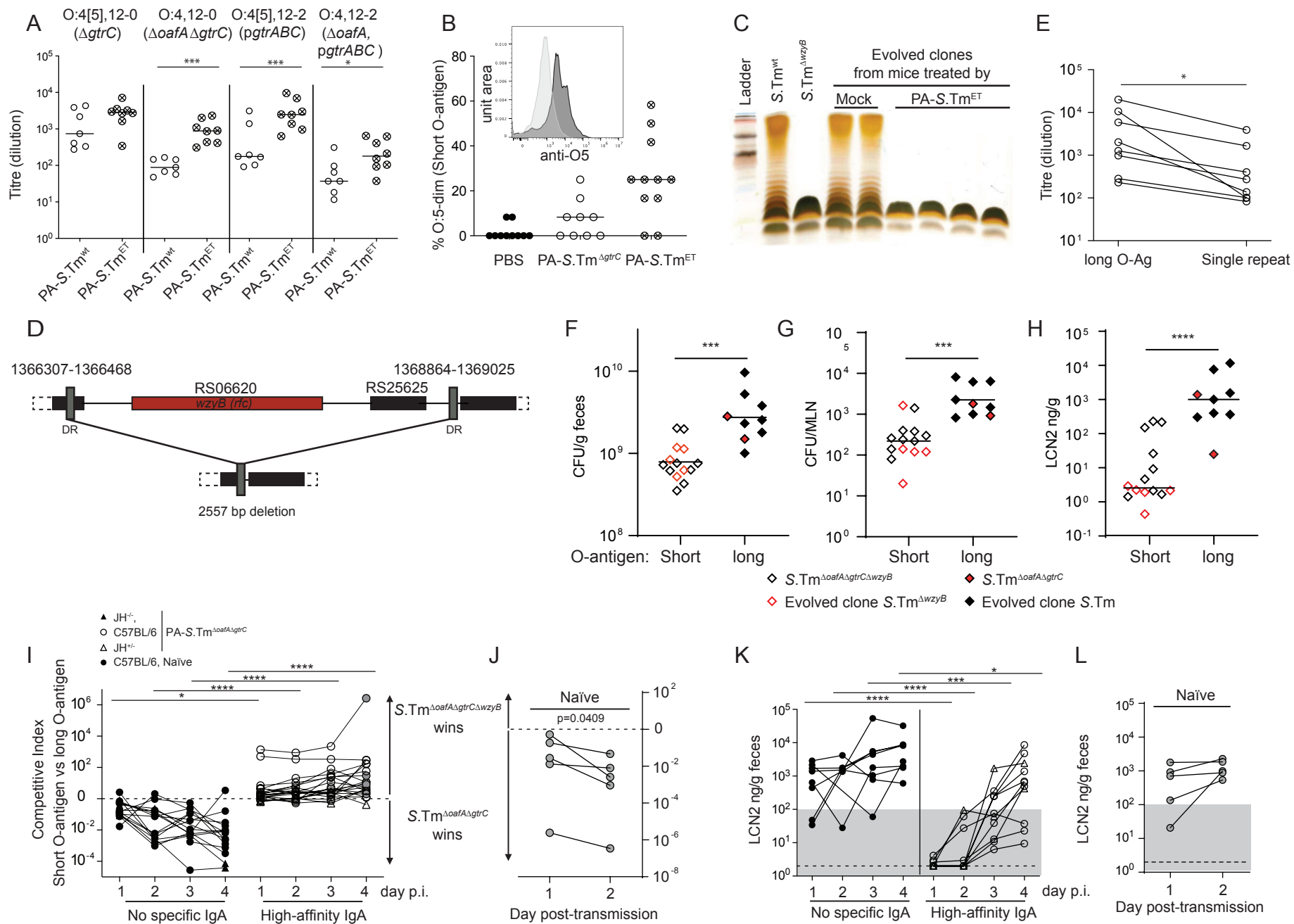


Figure 4: Induction of IgA against fitness-neutral glycan variants set an evolutionary trap for S.Tm, selecting for strains with a short O-antigen

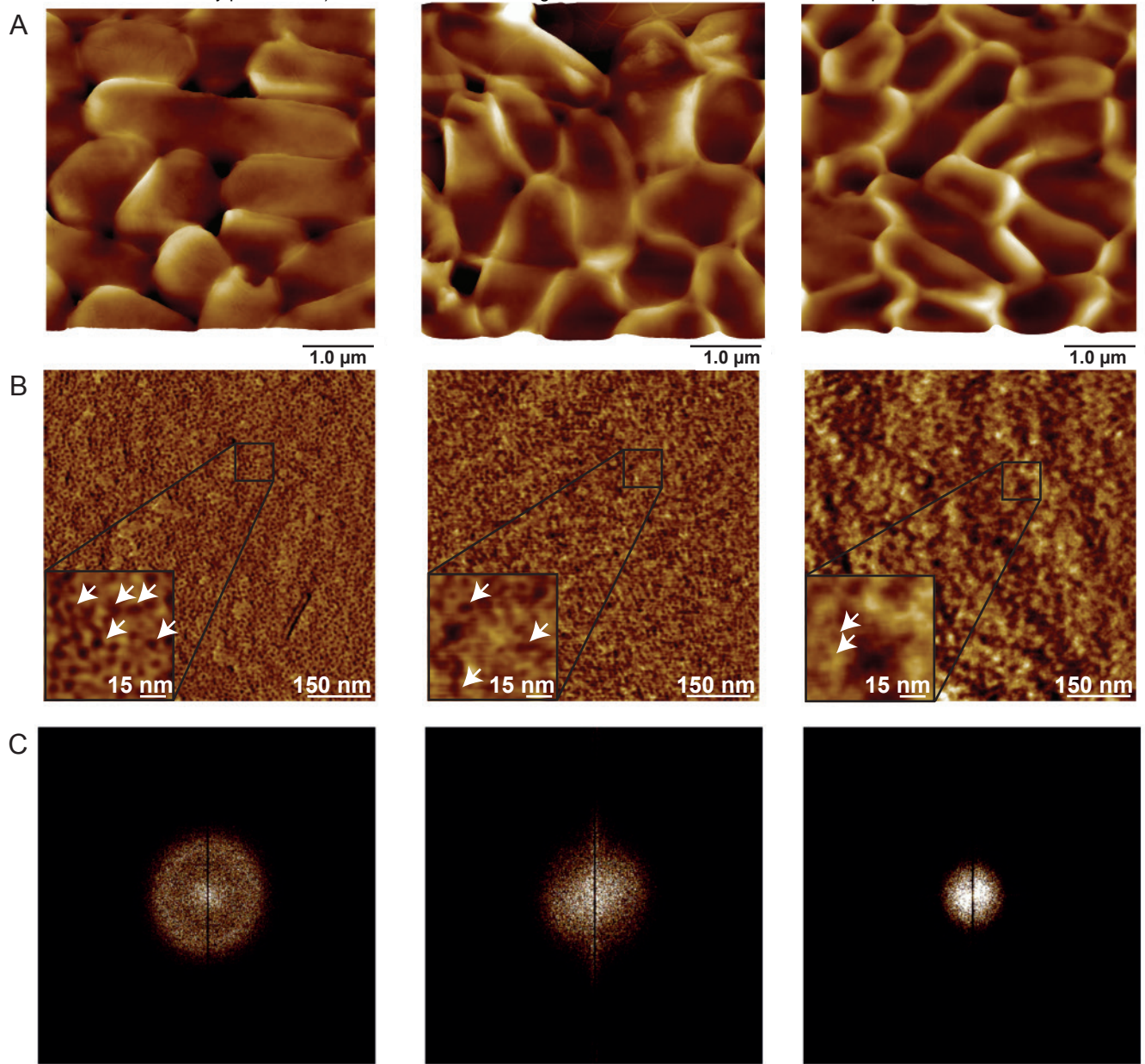


Fig. S1: Surface phenotype of *S.Tm* mutants

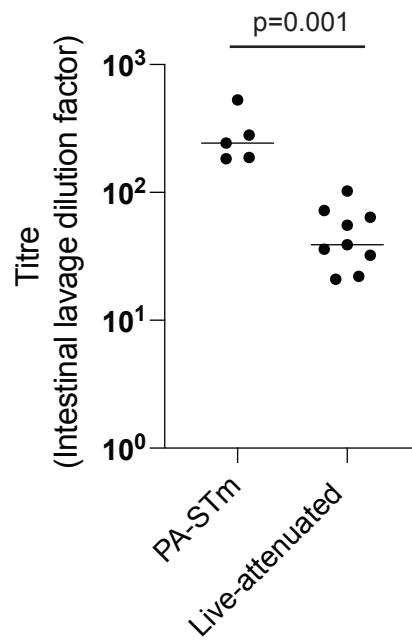


Figure S2: Inactivated oral vaccines induce higher titre IgA than chronic infection with live-attenuated (SPI2-deficient) *S.Tm* mutants.

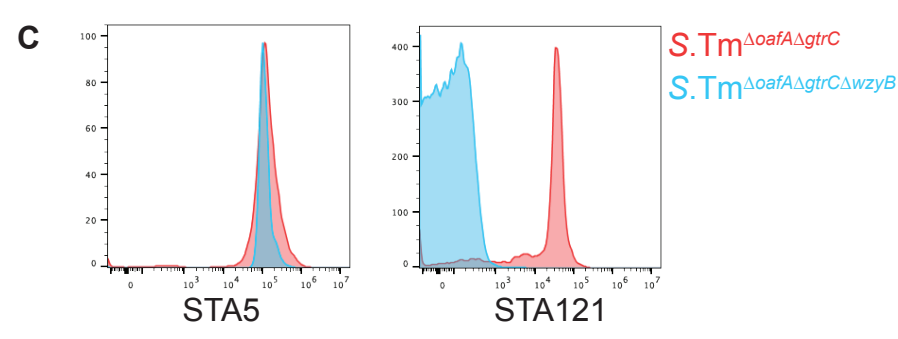
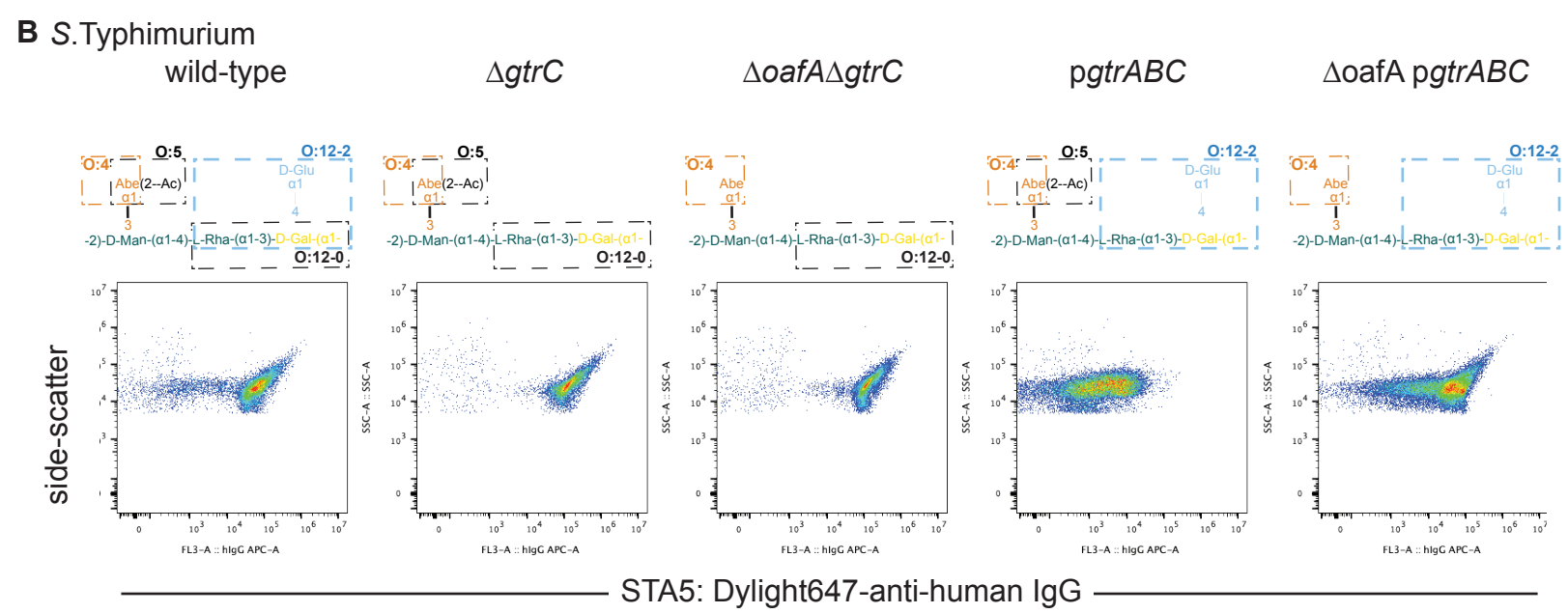
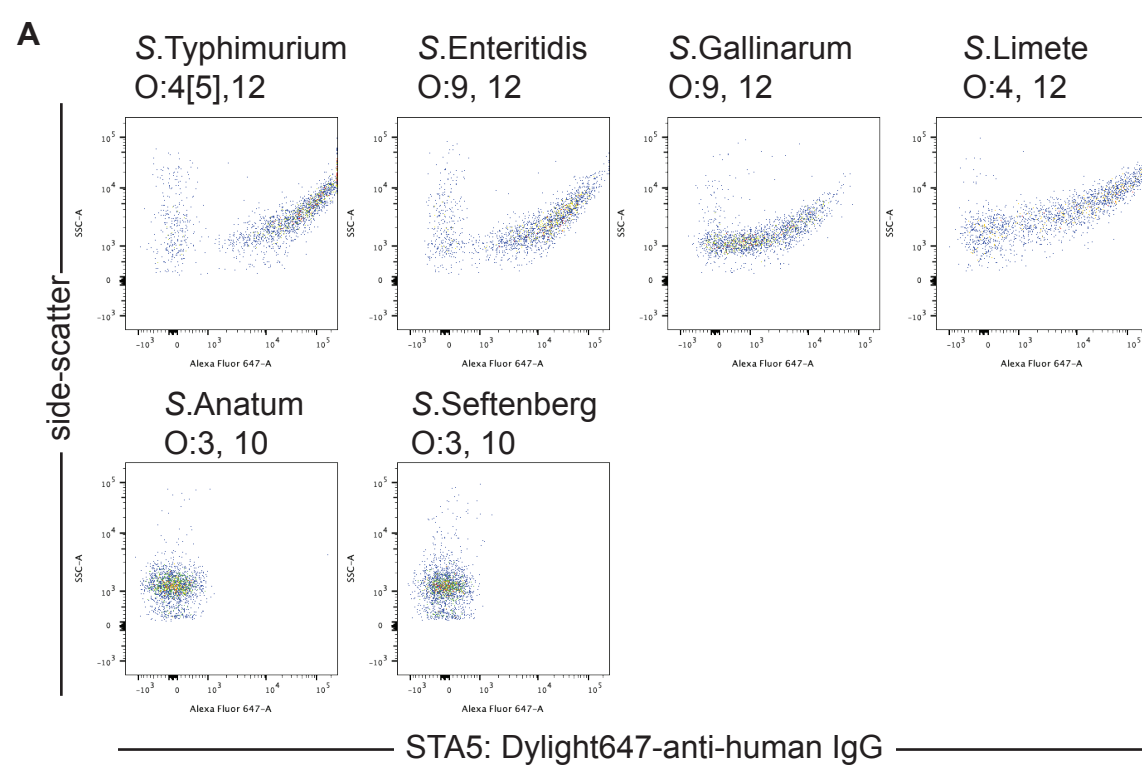
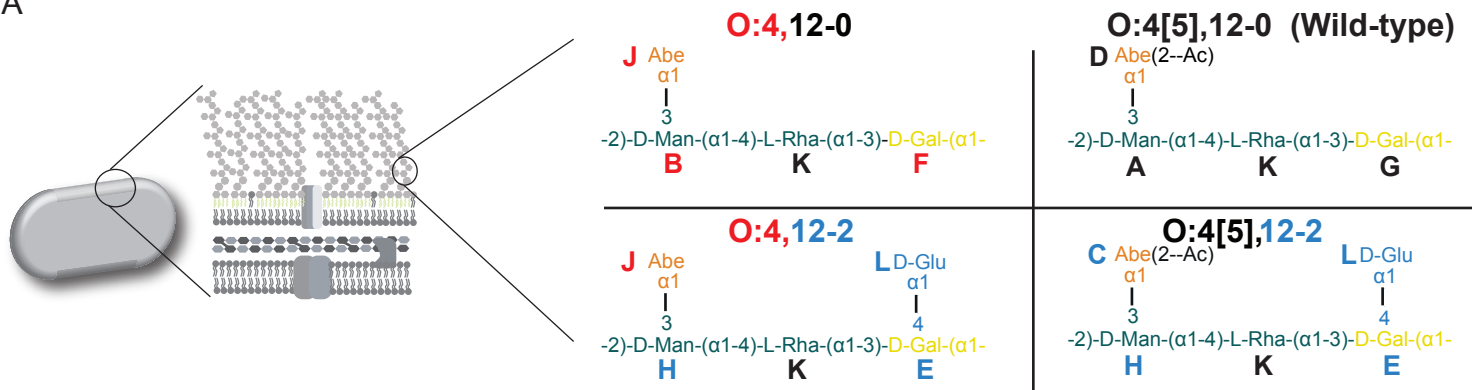
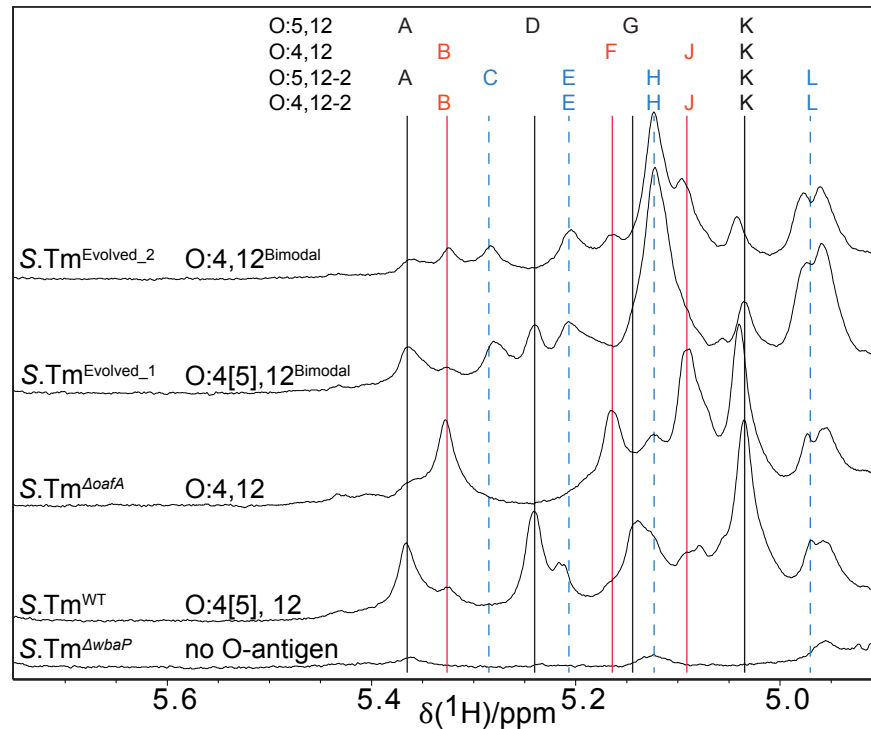


Figure S3: Characterization of the O:12-0 specificity of STA5 and STA121 using diverse *Salmonella enterica* serovars and recombinant *S. Tm* strains

A



B



C

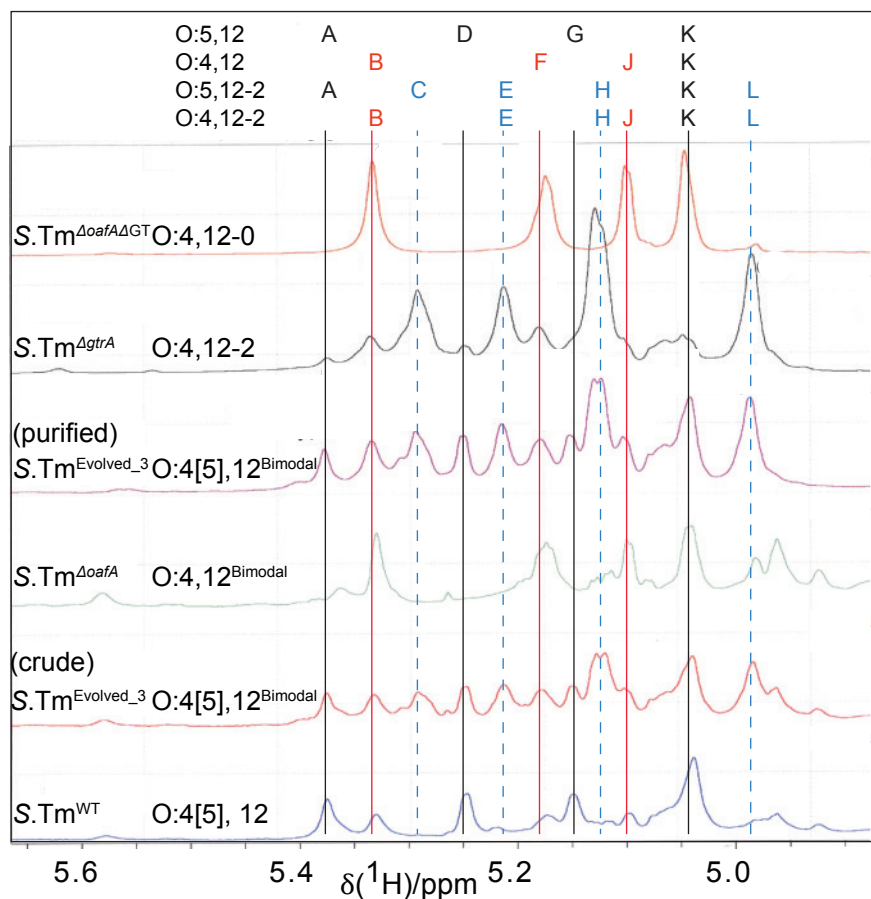


Fig. S4: NMR analysis of O-antigen structures.

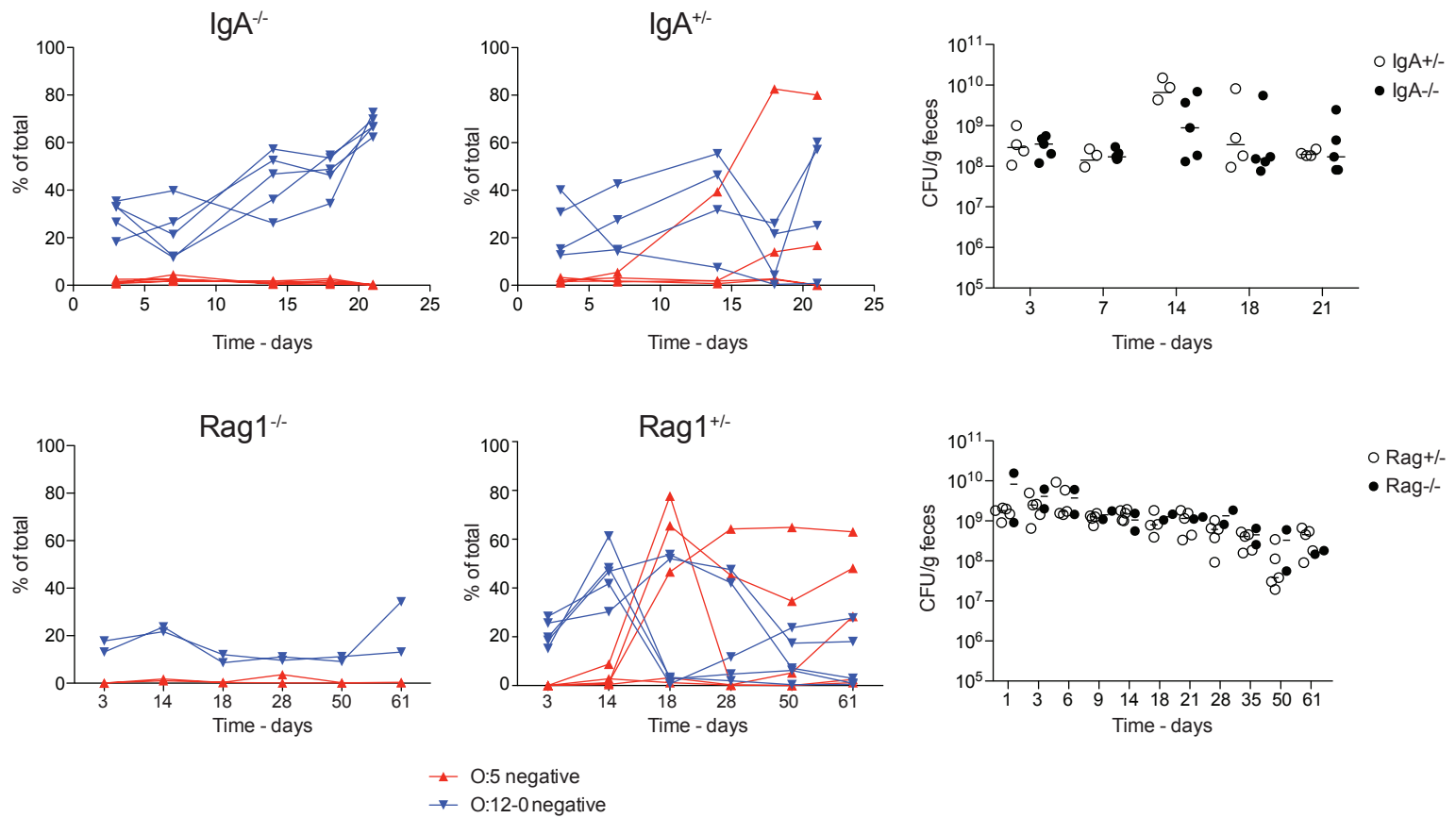


Fig S5: S.Tm clones with loss of abequose acetylation (O:5-negative) and loss of O:12-0-antibody binding due to glucosylation (O:12-0-negative) arise during chronic infections with attenuated S.Tm

Changes in O:12-0 anti-sera binding

Changes in O:5 anti-sera binding

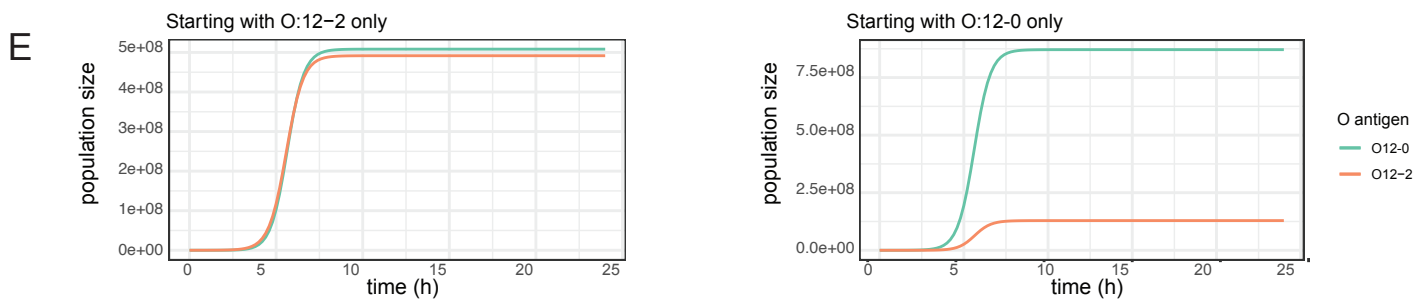
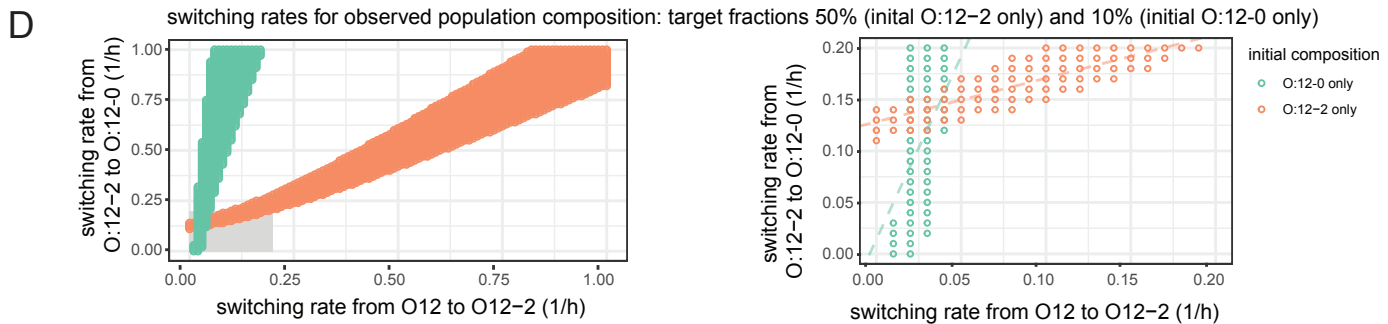
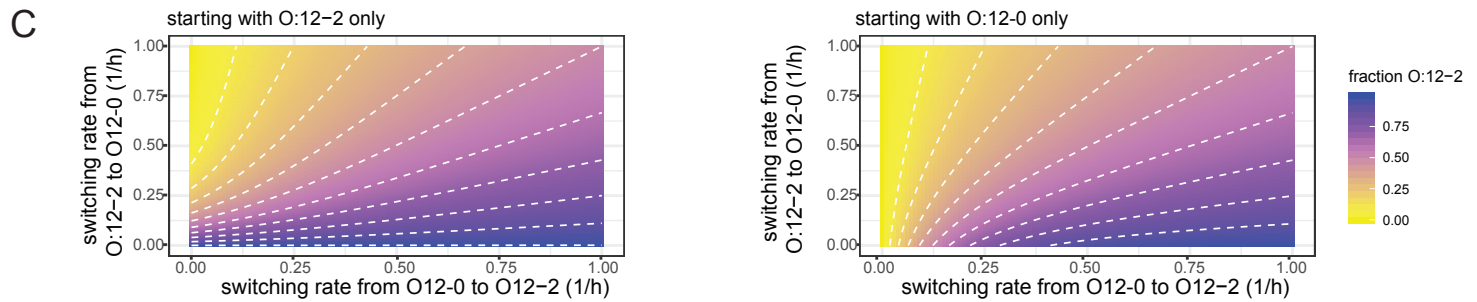
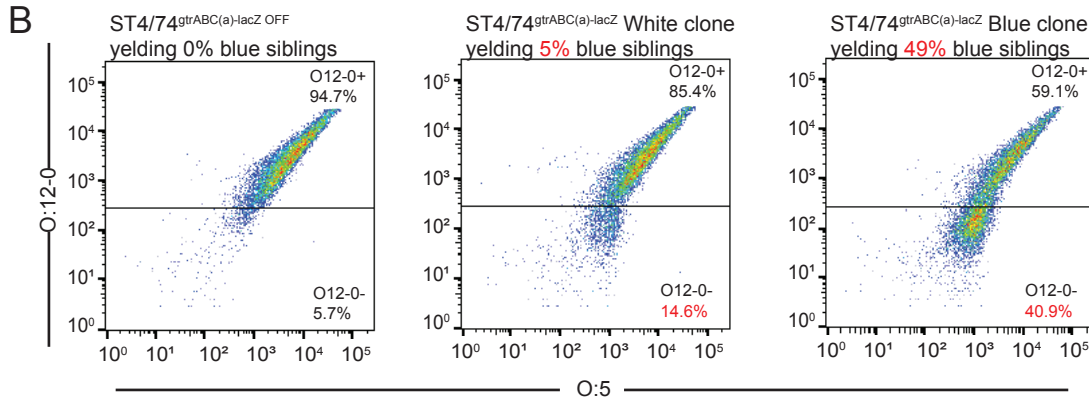
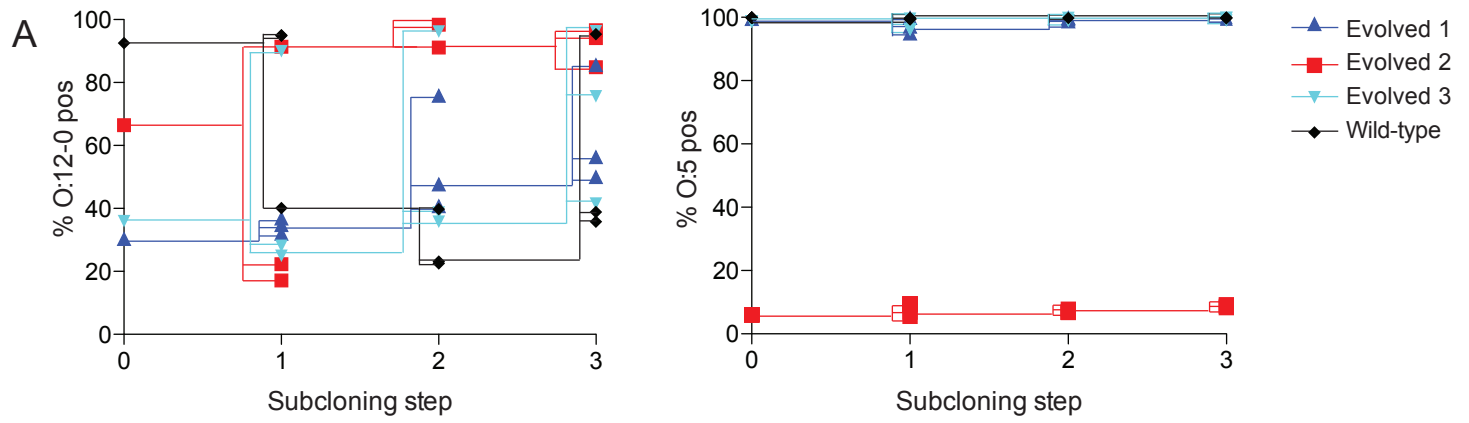
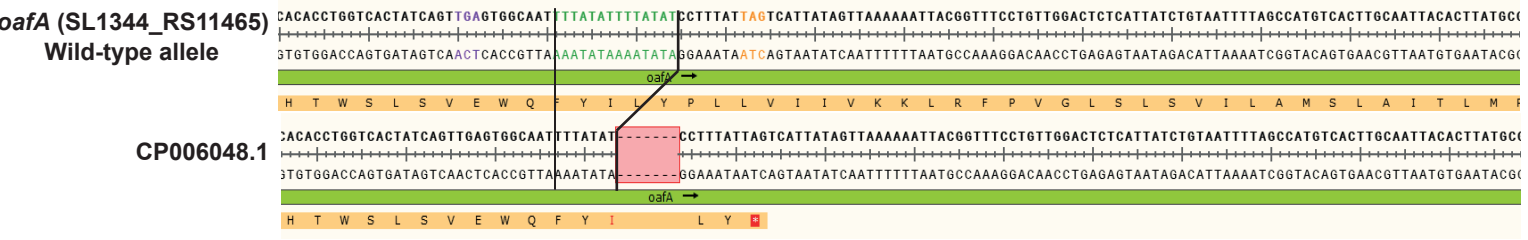


Fig. S6: Loss of O:12-0-staining is a reversible phenotype

A



B

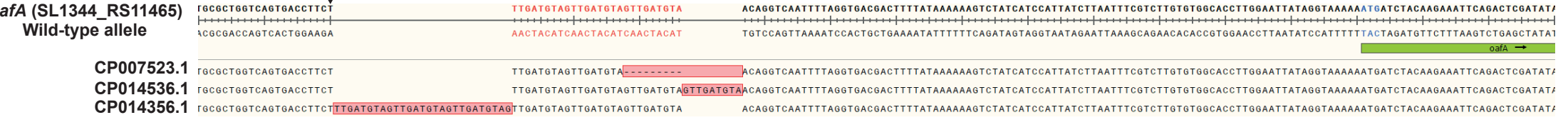


Fig. S7: Mutations detected in the oafA gene sequence among several strains of S. Tm

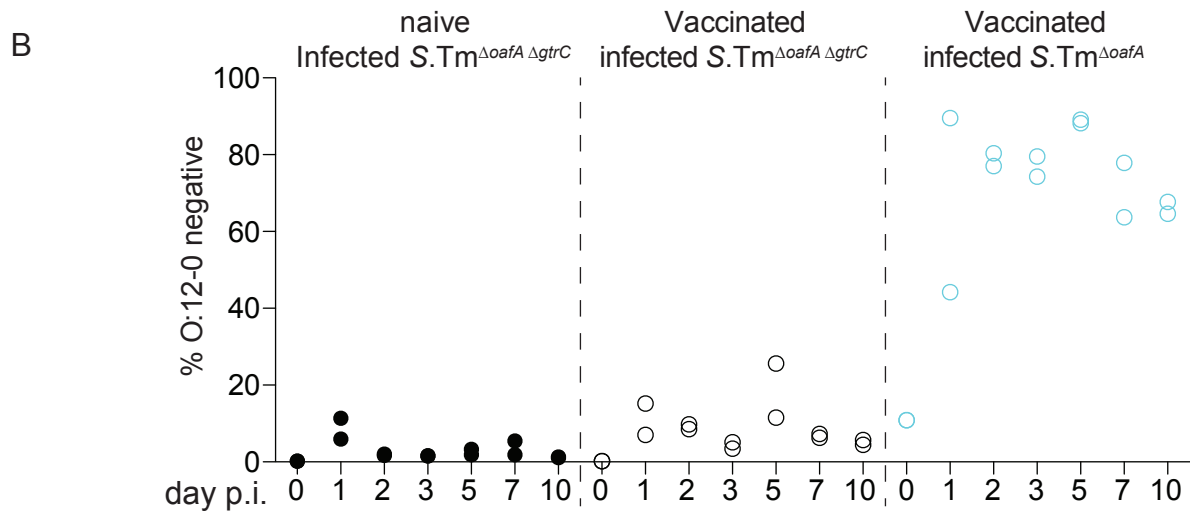
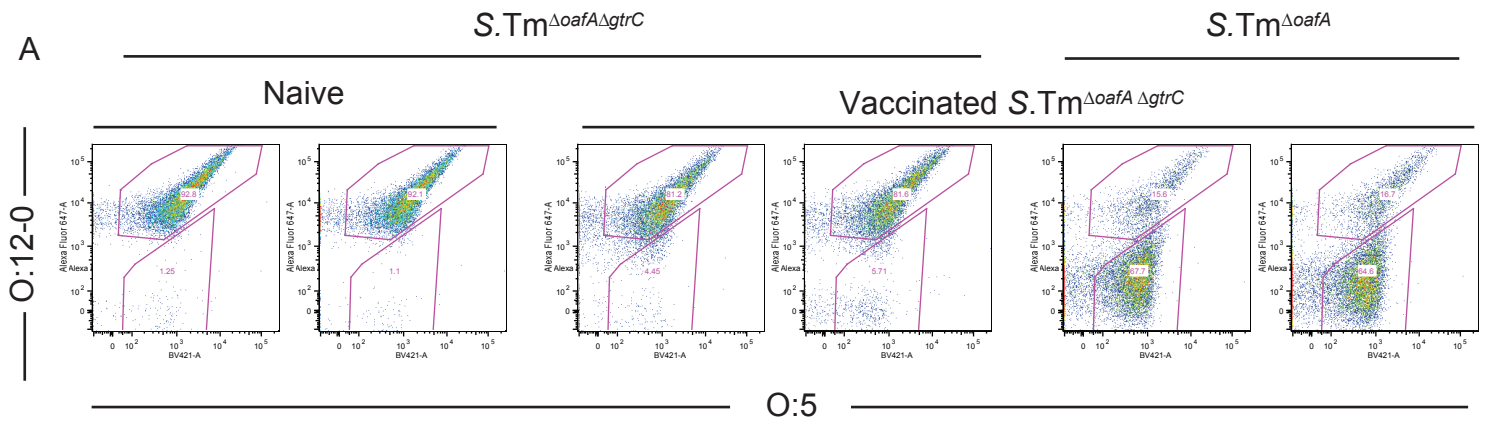


Fig. S8: *gtrC* is required for generation of the O12^{Bimodal} phenotype

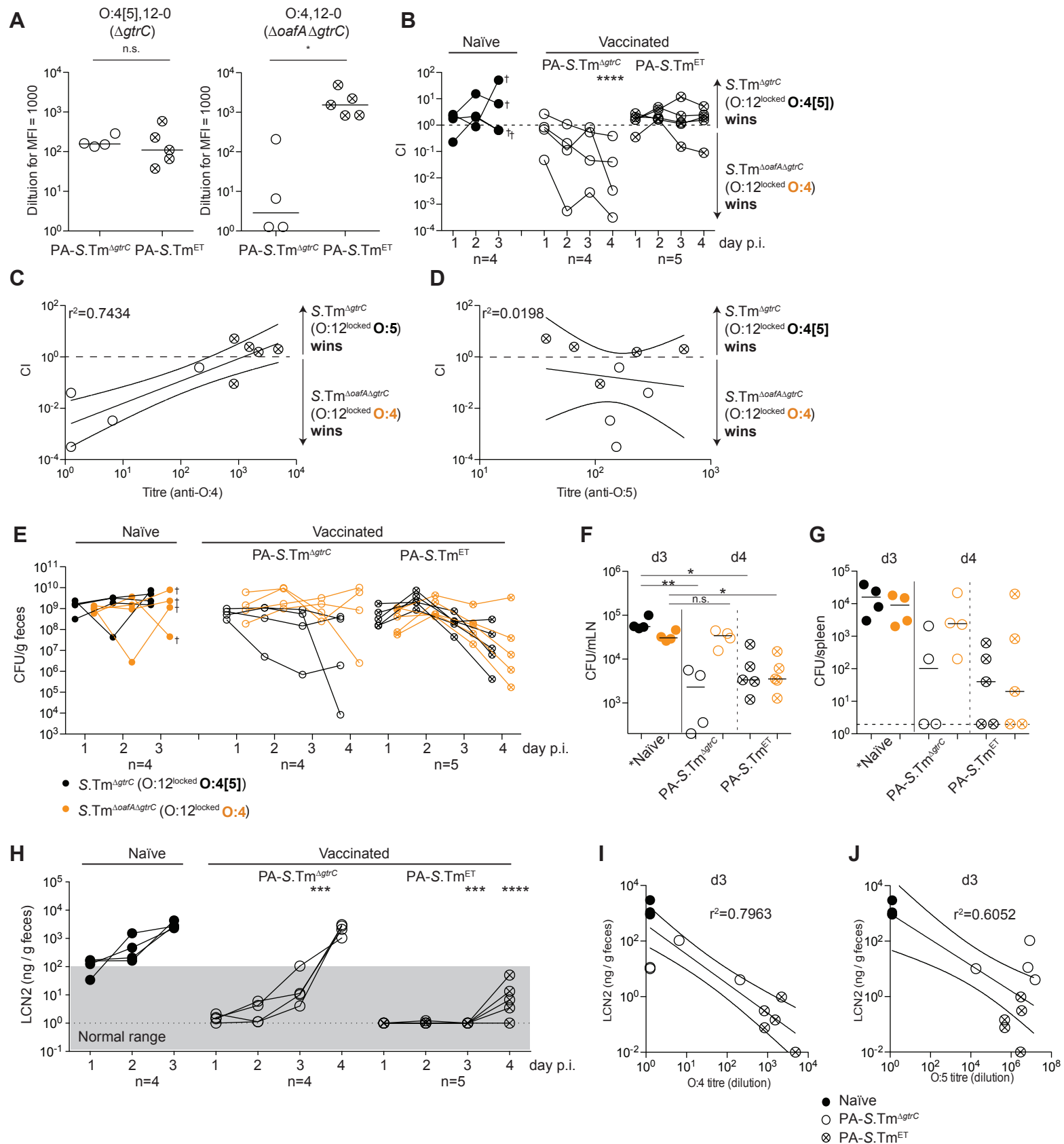


Figure S9: IgA-drive selective pressure and Evolutionary Trap Vaccines function identically in SPF Balb/c mice

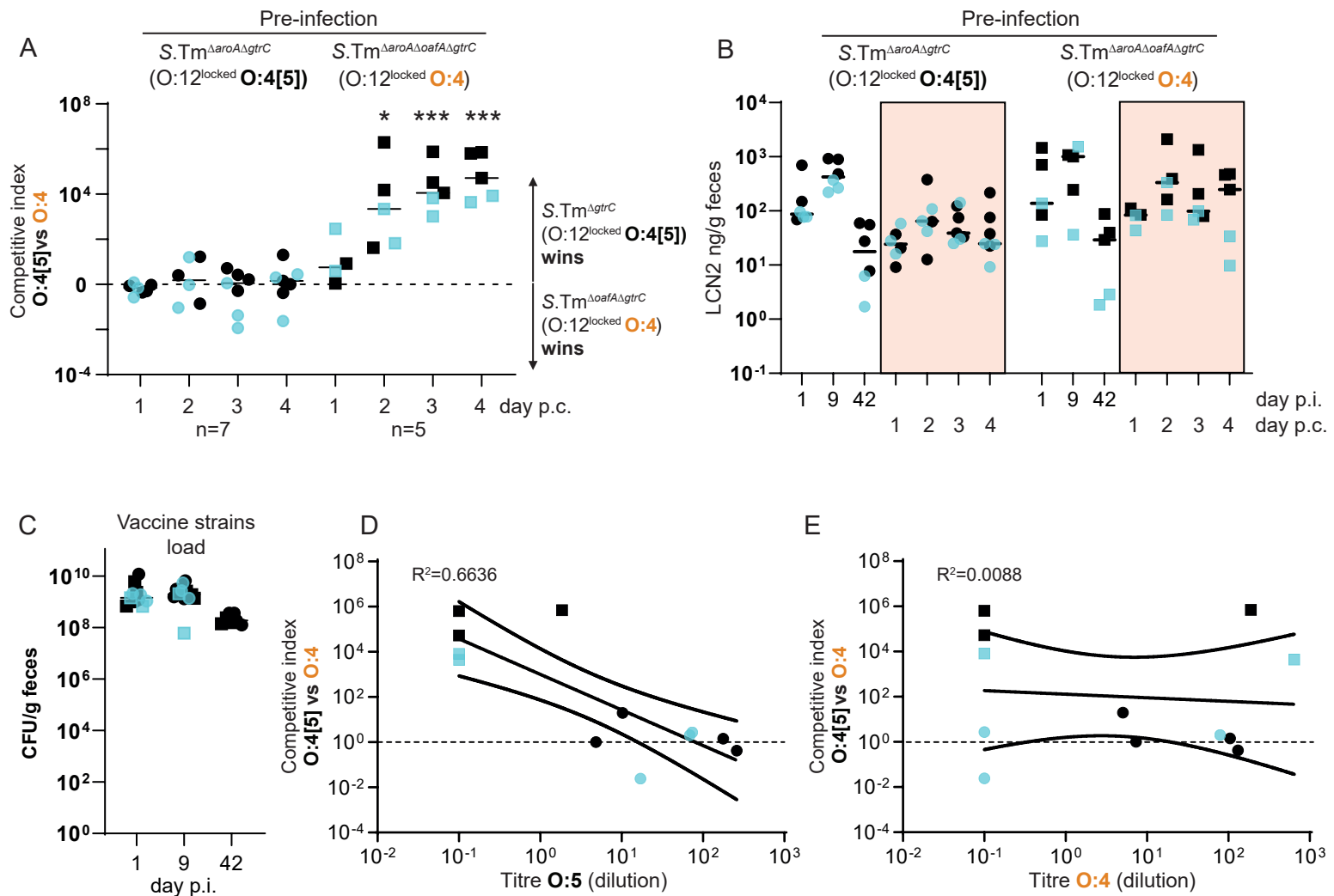


Figure S10: “Vaccination” by chronic infection with attenuated *aroA oafA* mutants but not with *aroA* mutants drives outcompetition of *OafA*-sufficient *Salmonella* on re-challenge, which correlates with O:5-specific antibody responses.

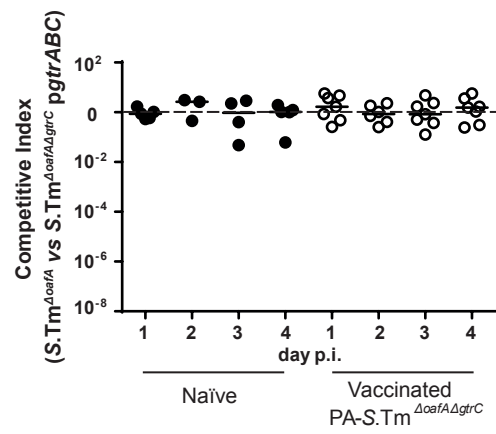


Fig S11: The Δ gtrC mutation can be complemented in trans

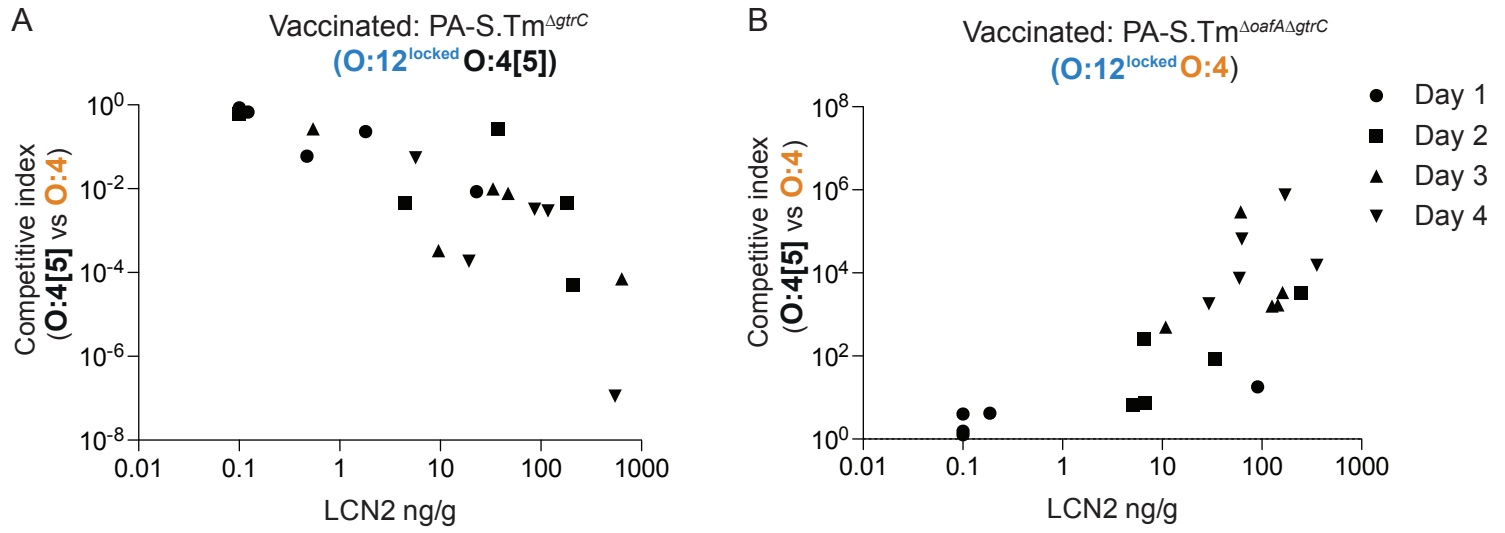


Fig S12: Fecal Lipocalin 2 measurements corresponding to figure 3A

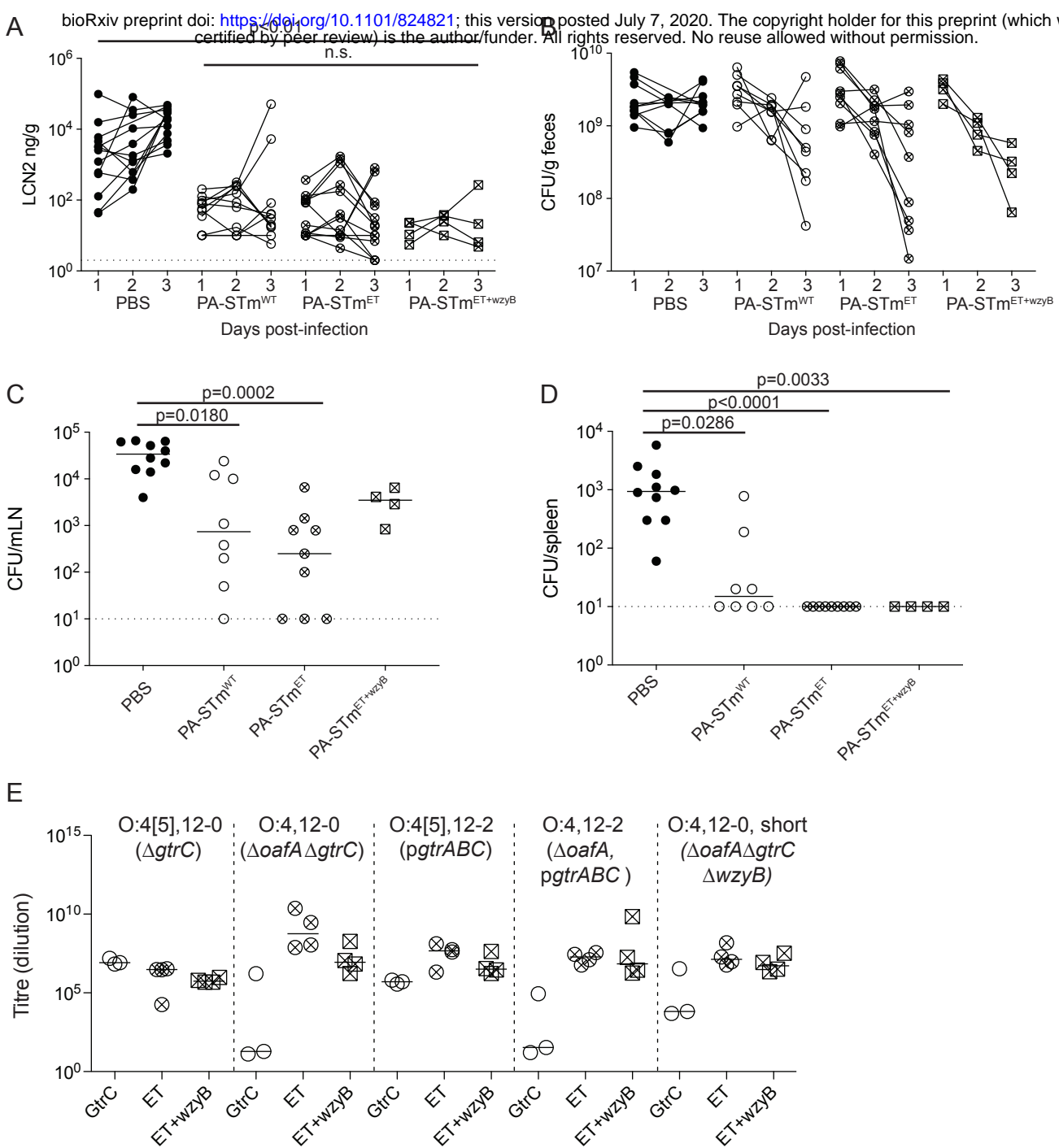


Fig. S13. PA-STm^{ET} does not significantly decrease inflammation or tissue invasion as compared to PA-STm^{WT}

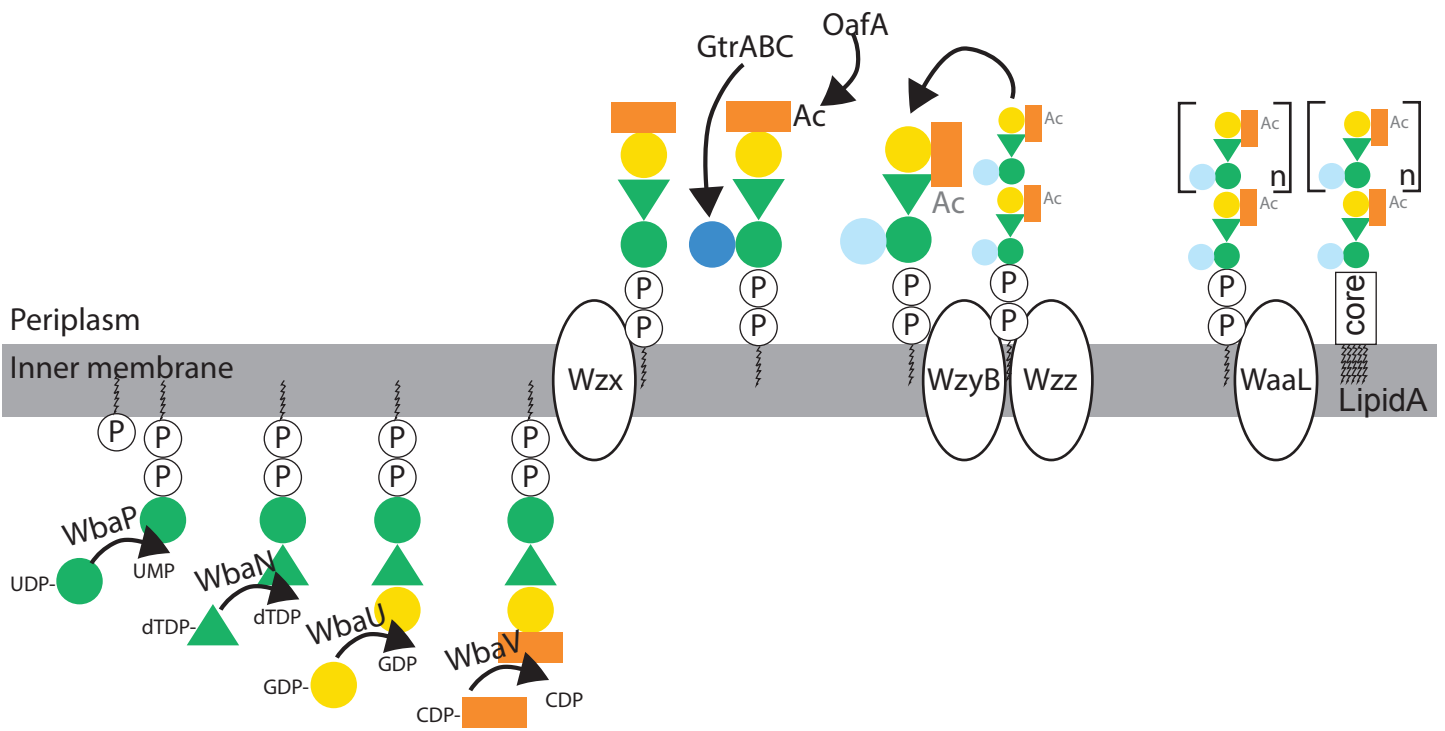


Fig. S14: Schematic diagram of O-antigen synthesis in *S.Tm*

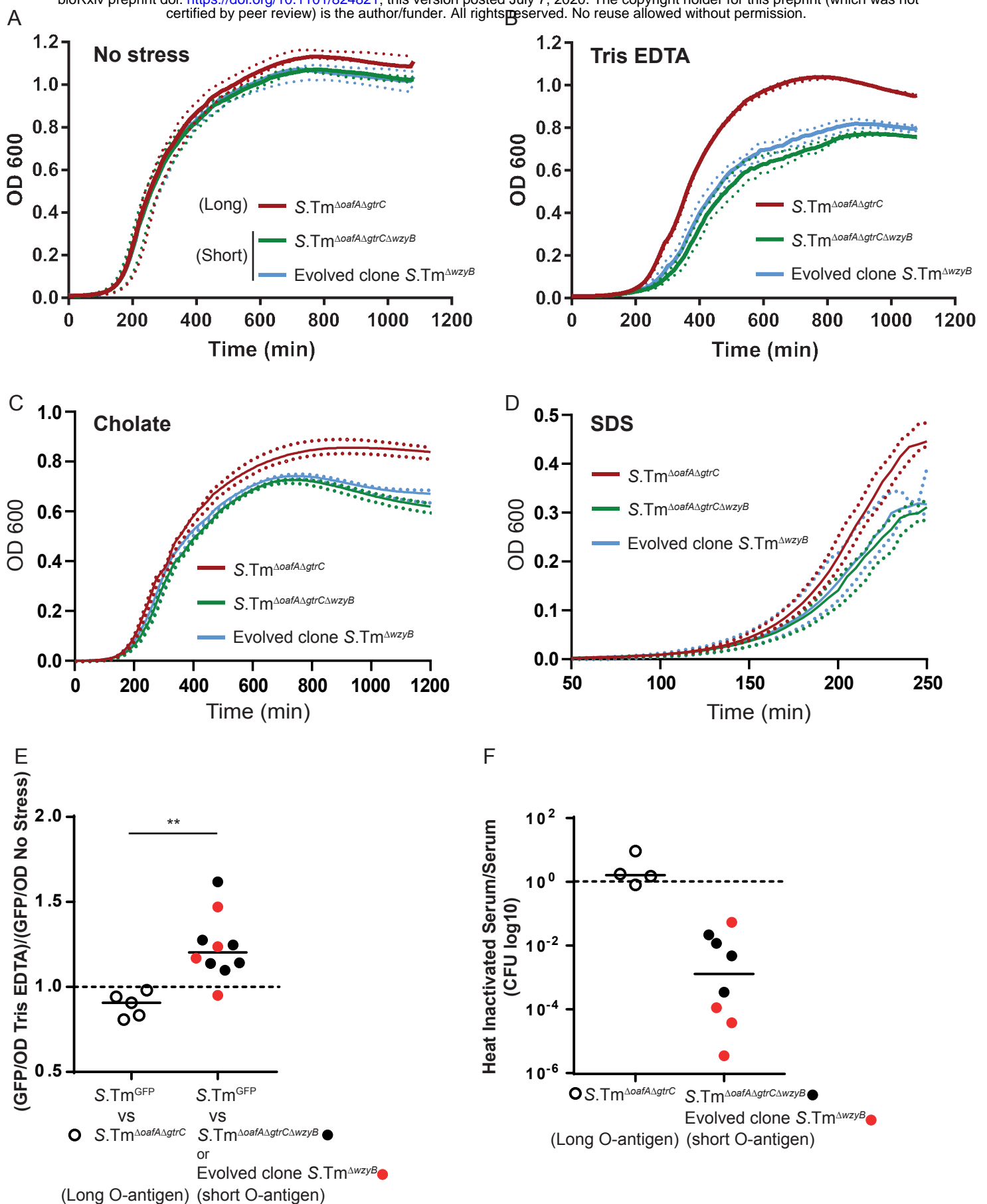


Fig S15: Synthetic and natural deletions of *wzyB* reduce the fitness of *S.Tm* in presence of Tris-EDTA, Cholate, SDS and serum complement

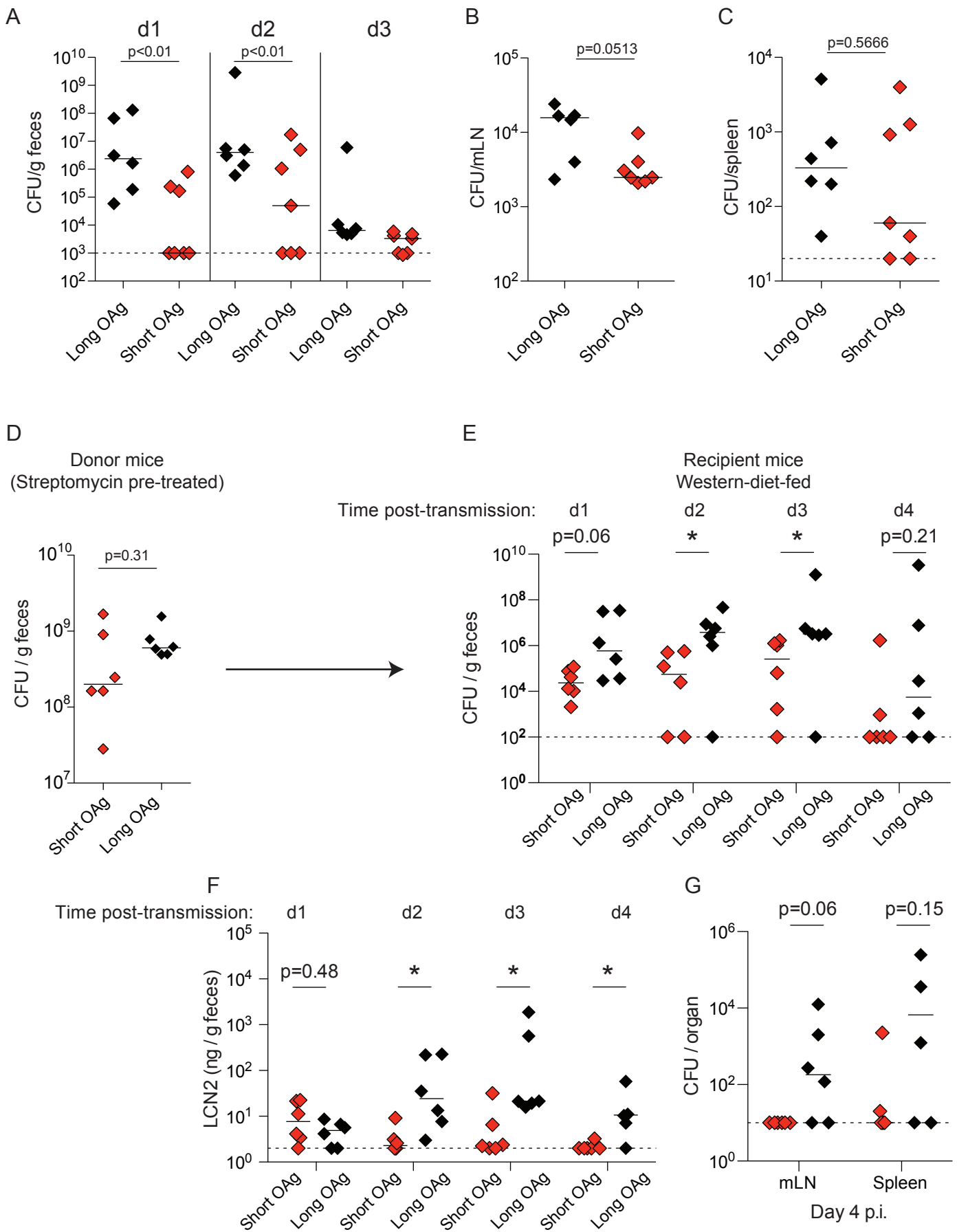
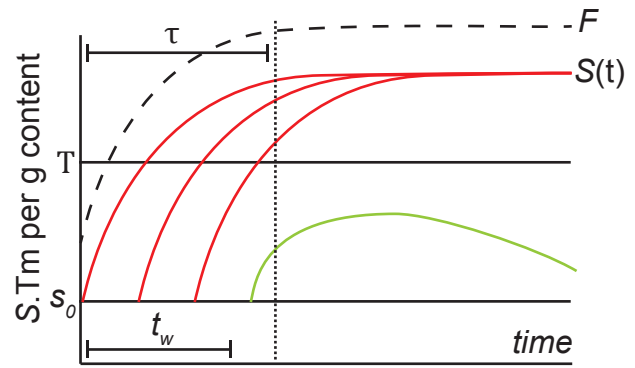
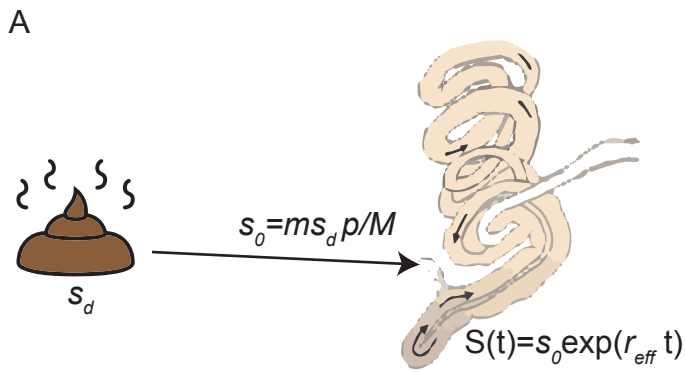


Figure S16: Short O-antigen *S.Tm* poorly colonizes the gut of western diet-fed mice, and fails to transmit between animals in this realistic disease model



- s_d Density of S.Tm in donor feces
- s_0 Density of S.Tm at start of infection in recipient
- m Mass of feces ingested
- p Probability of an S.Tm surviving from shedding to arrival in GIT of recipient
- M Mass of lower GIT content in recipient
- r_{eff} Net replication rate of S.Tm in recipient GIT
- t_w Time window during which successful transmission can be achieved
- T Threshold density of S.Tm required to drive inflammation and fulminant infection
- τ Duration of microbiota perturbation permitting S.Tm growth
- F Density of Microbiota

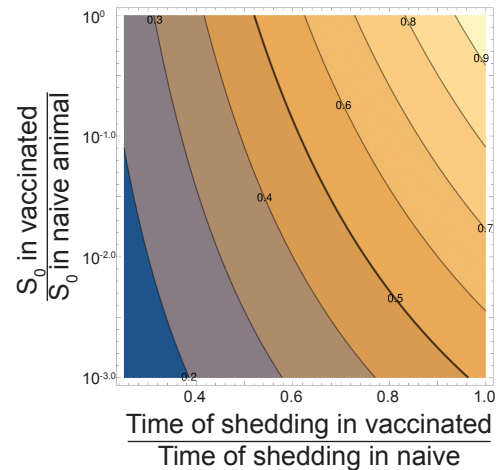
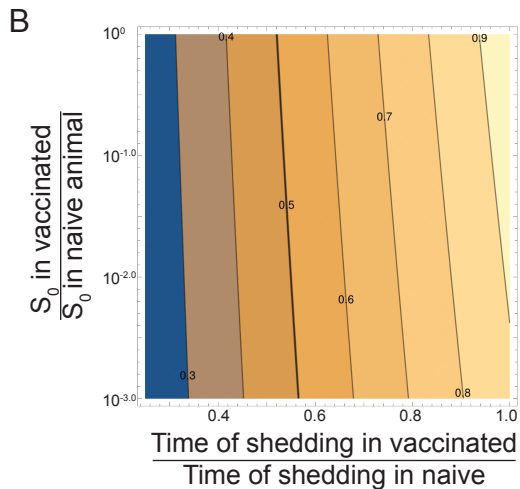
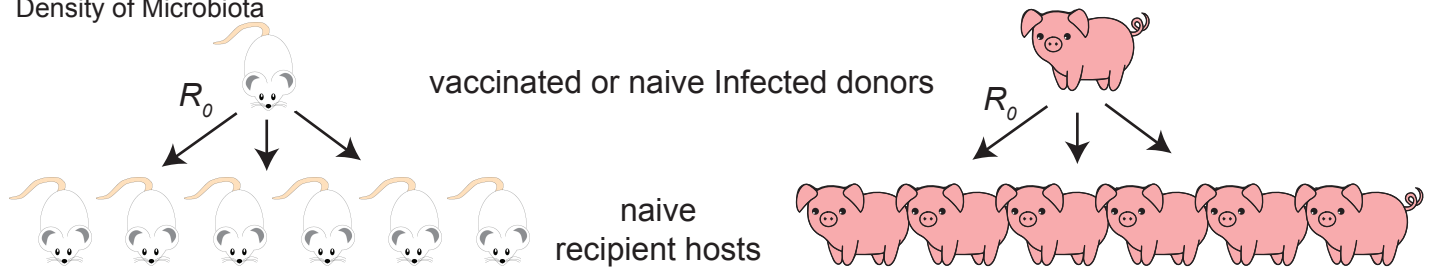





Figure S17: Mathematical model of S.Tm transmission in mice and in domestic pigs

Serovar	Full Representation	SNFG Representation
<p>O:4[5],12-0</p>	<p style="text-align: center;">O:5</p> <p style="text-align: center;">Abe(2--Ac) α1</p> <p style="text-align: center;"> 3</p> <p style="text-align: center;">-2)-D-Man-(α1-4)-L-Rha-(α1-3)-D-Gal-(α1-</p> <p style="text-align: right;">O:12-0</p>	
<p>O:4,12-0</p>	<p style="text-align: center;">O:4 Abe α1</p> <p style="text-align: center;"> 3</p> <p style="text-align: center;">-2)-D-Man-(α1-4)-L-Rha-(α1-3)-D-Gal-(α1-</p> <p style="text-align: right;">O:12-0</p>	
<p>O:4[5],12-2</p>	<p style="text-align: center;">O:5</p> <p style="text-align: center;">Abe(2--Ac) α1</p> <p style="text-align: center;"> 3</p> <p style="text-align: center;">-2)-D-Man-(α1-4)-L-Rha-(α1-3)-D-Gal-(α1-</p> <p style="text-align: right;">O:12-2</p> <p style="text-align: right;">D-Glu α1 4</p>	
<p>O:4,12-2</p>	<p style="text-align: center;">O:4 Abe α1</p> <p style="text-align: center;"> 3</p> <p style="text-align: center;">-2)-D-Man-(α1-4)-L-Rha-(α1-3)-D-Gal-(α1-</p> <p style="text-align: right;">O:12-2</p> <p style="text-align: right;">D-Glu α1 4</p>	